

# Summary of the final report for the research project:

## Investigation of Membrane Fouling in the Treatment of Oily Wastewater (W-UFO)

For the Sub-project

**W-UFO III<sup>+</sup>:** Influence of dissolved oil and process optimization  
(01.2022 – 03.2024)



## Team:

**University of Duisburg-Essen**  
**Faculty of Engineering**  
**Department of Mechanical Engineering and Process Engineering**  
**Chair of Mechanical Process Engineering / Water Technology**

Lotharstr. 1  
47057 Duisburg  
[www.uni-due.de/wassertechnik/](http://www.uni-due.de/wassertechnik/)

Prof. Dr.-Ing. Stefan Panglisch (Project PI)  
Telefon: 0203 379 -3477  
[stefan.panglisch@uni-due.de](mailto:stefan.panglisch@uni-due.de)

Dr. Ibrahim ElSherbiny  
[ibrahim.elsherbiny@uni-due.de](mailto:ibrahim.elsherbiny@uni-due.de)

M.Sc. Hasan Idrees (PhD Student)  
[hasan.idrees@uni-due.de](mailto:hasan.idrees@uni-due.de)

**The project was funded by**  
**Willy-Hager-Stiftung**  
**c/o Technische Universität Kaiserslautern**  
**Paul-Ehrlich-Straße 14**  
**67663 Kaiserslautern**

Contact:  
Prof. Dr.-Ing. Heidrun Steinmetz

## Table of Contents

<b>Table of Contents</b>	<b>III</b>
<b>1 Deutsche Zusammenfassung</b>	<b>4</b>
1.1 Einleitung und Zielsetzung	4
1.2 Zusammenfassung der Ergebnisse	5
1.3 Fortschritte und Änderungen des ursprünglichen Zeitplans	9
1.4 Veröffentlichungen	14
<b>2 Summary of the main scientific outputs</b>	<b>15</b>
2.1 Literature review	15
2.1.1 Protocols for the production of synthetic oily wastewater effluents	15
2.1.2 Management of produced water	15
2.1.3 Environmental and economic assessment	18
2.2 Materials and Methods	19
2.2.1 Chemicals	19
2.2.2 Membranes	19
2.2.3 Preparation of emulsified oil	20
2.2.4 Characterization of the emulsified oils	20
2.2.5 Adsorption experiments	21
2.2.6 Coagulation/flocculation jar-test experiments	22
2.2.7 Dead-end filtration experiments	22
2.2.8 Hybrid UF tests with the dosage of PAC and/or coagulants	22
2.2.9 Semi-technical length and long-term hybrid filtration experiments	22
2.2.10 Environmental and economic assessment	23
2.3 Results and discussion	23
2.3.1 Contribution of water-soluble oil fraction in the membrane fouling	23
2.3.2 Further investigations on the surfactant-enhanced dead-end UF	27
2.3.3 Hybrid UF processes with PAC dosing and/or coagulants	43
2.3.4 Experiments relevant to practice	51
<b>3 Conclusion and outlook</b>	<b>55</b>
<b>4 References</b>	<b>58</b>
<b>5 Appendices</b>	<b>62</b>
5.1 List of Abbreviations	62
5.2 List of Figures	63
5.3 List of Tables	66

# 1 Deutsche Zusammenfassung

## 1.1 Einleitung und Zielsetzung

Das finale Ziel der W-UFO-Forschungsprojektreihe ist die Entwicklung eines effizienten, druckgesteuerten, membranbasierten Aufbereitungsprozesses als Tertiärbehandlung (d.h. Polishing) für Produced Water (PW; typisches Abwasser aus der Öl- und Gasindustrie). In den primären und sekundären Behandlungsstufen werden in der Regel Schwebstoffe und große Öltröpfchen abgetrennt, so dass das behandelte PW eine Ölkonzentration im Bereich von 20 – 100 mg/L sowie Öltröpfchengrößen  $< 20 \mu\text{m}$  aufweist. Ein effizientes Dead-End-Filtrationsprotokoll, bei dem typische polymere Hohlfaser-Ultrafiltrationsmembranen (UF) zum Einsatz kommen, kann das bereits gut erforschte Cross-Flow-Verfahren ersetzen, da es eine höhere Reinwasserproduktivität, einen geringeren Energiebedarf und somit niedrigere Betriebskosten bietet. Für weitere Details zur Problemdefinition siehe Abschnitt 1.1, Seite 6, im finalen W-UFO-Bericht.

Das Projekt W-UFO III<sup>+</sup> ist das dritte und letzte Teilprojekt der W-UFO-Forschungsprojektreihe. Es zielt darauf ab, die Auswirkungen der gelösten Ölfraction im PW auf das Wachstum des Membranfoulings und die Permeatqualität zu verstehen sowie die Optimierung und Kostenbewertung des entwickelten Tensid-unterstützten Dead-End-Membranfiltrationsprozesses durchzuführen. Bei W-UFO II wurde festgestellt, dass die Dosierung eines anionischen Tensids (d.h. Natriumdodecylsulfat, SDS) vor der Membranfiltration die Reversibilität von Fouling deutlich erhöhen und die hydraulische Rückspülbarkeit im Dead-End-UF-Verfahren verbessern konnte. Dies ermöglichte die Filtration von emulgiertem Öl mit Ölkonzentrationen von bis zu 50 mg/L, eine Konzentration, von der in der Literatur für Dead-End Verfahren bisher nicht berichtet wurde. Dennoch hat das neu entwickelte, SDS-unterstützte UF-Verfahren auch Bedenken hinsichtlich der Kosteneffizienz, der Einleitungsbestimmungen (da das Tensid nicht vollständig von der Membran zurückgehalten werden kann), zuverlässiger Optionen für die Wiederverwendung des Wassers (z.B. als Prozesswasser) sowie der Anwendbarkeit auf andere ölhaltige Abwässer aufgeworfen. Diese Bedenken (oder Fragen) waren die Motivation für das W-UFO III<sup>+</sup> Projekt. Zum W-UFO III<sup>+</sup>-Plan gehört auch die Untersuchung der Anwendbarkeit von Hybrid-UF-Prozessen, wie der Kombination mit Pulveraktivkohle (PAC) oder Koagulation: PAC-UF, Koagulation-UF und PAC-Koagulation-UF. Für weitere Details zur Projektziele, Vorgehensweise

sowie entwickelte Hypothesen vergleiche Abschnitte 1.2, 1.3 und 1.4 in Seiten 9, 11 und 13 im finalen W-UFO-Bericht.

Das W-UFO III+ Projekt umfasst fünf Arbeitspakete (WP): Quantitative Bestimmung der gelösten Ölfractionen (WSO) und Untersuchung ihres Einflusses auf die Membranleistung und die Fouling-Mechanismen (WP 1), Optimierung des Aufbereitungsprozesses (WP 2), Validierung des entwickelten Aufbereitungsprotokolls und Anwendbarkeit auf andere Arten von Produced Water (WP 3), Bewertung der Kosten und potenziellen Umweltauswirkungen der SDS-Dosierung (WP 4) und Langzeitexperimente mit Modulen im Labormaßstab mit technischer Länge (WP 5). Für weitere Details zum Arbeitsplan von W-UFO III+ sehe den überarbeiteten W-UFO III+ -Antrag Abschnitt 5.4, Seite 18.

## 1.2 Zusammenfassung der Ergebnisse

Die Untersuchungen im W-UFO III+ Projekt wurden in vier Themen unterteilt: (1) Untersuchung des Beitrags der WSO zum Membran-Fouling, (2) Weitere Untersuchung der Effizienz der im W-UFO II-Projekt entwickelten Tensid-unterstützten Dead-End-UF. (3) Untersuchung der Anwendbarkeit von Hybrid-UF-Prozessen, wie der Kombination mit PAC oder Koagulation: PAC-UF, Koagulation-UF und PAC-Koagulation-UF. (4) Praxisrelevante Experimente zur Skalierbarkeit der Ergebnisse auf längeren Membranmodulen mit größerer aktiver Oberfläche und Durchführung langfristiger Filtrationsversuche.

1. Mehrere Methoden wurden zur Trennung und Bestimmung der WSO in emulgierten Ölen und deren Einfluss auf die Leistung und Fouling von UF-Membranen untersucht. Drei analytische Techniken basierend auf Extrahierung und Analyse mit GC-MS oder Fluoreszenz-Anregungs-Emissions-Matrix (FEEM) wurden etabliert und implementiert. Emulgierte Öle wurden durch Membranen mit Porengrößen von 0,1, 0,2 und 0,45  $\mu\text{m}$  filtriert und die resultierenden Permeate weiter durch kapillare UF-Membranen filtriert. Die emulgierten Öle, die Permeate der 0,1, 0,2 und 0,45  $\mu\text{m}$  Membranen sowie das Permeat der UF-Membranen wurden auf ihren WSO-Gehalt analysiert. Unsere Experimente zeigten, dass WSO unter den getesteten Bedingungen nicht signifikant zum Fouling der UF-Membran durch emulgierte Öle beitrugen.

2. Die weitere Untersuchung der Effizienz der Tensid-unterstützten Dead-End-UF umfasste: (a) Untersuchungen zur Definition des Wirkmechanismus von SDS bei Zugabe zu emulgierten Ölen vor der UF, die zu einer verbesserten BW-Effizienz führte. (b) Quantitative Bestimmung der SDS-Konzentration in UF-Permeaten. (c) Einfluss der Qualität des verwendeten SDS. (d) Optimierung der Betriebsbedingungen, einschließlich Filtrationsfluss, Filtrationsdauer, BW-Fluss und BW-Dauer. (e) Wirtschaftliche und ökologische Bewertung der Tensid-unterstützten Dead-End-UF-Methode.
  - a. Drei Effekte wurden als gemeinsam verantwortlich für die geförderte hydraulische Fouling-Reversibilität und die erheblich verbesserte mechanische Rückspüleffizienz durch SDS-Zugabe vor der Membranfiltration identifiziert: (i) die Modifikation der emulgierten Öltröpfchen, die die Stabilität der Öltröpfchen während der Membranfiltration erhöhte und eine Koaleszenz in der Membrannähe verhinderte. (ii) die Adsorption von SDS-Monomeren in die polyethersulfone (PES) Membranmatrix (unterhalb der kritischen Mizellbildungskonzentration, CMC) induzierte eine Hydrophilisierung der Membranoberfläche und schwächte die Öladhäsion, indem hydrophobe Wechselwirkungen minimiert wurden. (iii) die Tensid-Monomere in der gebildeten Fouling-Schicht (sowohl an der Membranoberfläche adsorbiert als auch an emulgierten Öltröpfchen) förderten den Zugang von Rückspülwasser durch die Fouling-Schicht, reduzierten die Grenzflächenspannung zwischen Öl und Wasser und verbesserten somit die Rückspüleffizienz.
  - b. Die Bestimmung der SDS-Konzentration im Permeat der UF-Membran stellte eine Herausforderung dar. Vier Methoden wurden basierend auf der Literatur untersucht: TOC, Ionenchromatographie, Leitfähigkeit und spektrophotometrische Analyse. Jede Methode wies bei der Replikation in unserem Labor Schwierigkeiten und Nachteile auf. Die TOC-Analyse war aufgrund von SDS-induziertem Schaum ungenau. Die Ionenchromatographie konnte Dodecylsulfat nicht nachweisen und wurde durch SDS-Verunreinigungen gestört. Die Leitfähigkeit maß die SDS-Löslichkeit in Feed-Lösungen, war jedoch für Permeatproben aufgrund nicht zurückgehaltener

Natriumionen ungeeignet. Die spektrophotometrische Methode mit Stain-all-Farbstoff und UV-Absorption zeigte, dass SDS nicht von der UF-Membran zurückgehalten wurde.

- c. Während des W-UFO-Projekts wurden drei SDS-Produkte verwendet: SDS<sub>VWR,21</sub> (beschafft von VWR International, Belgien im Jahr 2021), SDS<sub>VWR,23</sub> (beschafft von VWR International, Belgien im Jahr 2023) und SDS<sub>TS</sub> (beschafft von Thermo Scientific, Indien). Bei der Filtration von SDS-modifizierten emulgierten Ölen und ölfreien SDS-Lösungen wurden bemerkenswerte Unterschiede im Membran-Fouling beobachtet. Der SDS-Qualität wurde mittels Elementaranalyse, FTIR-Spektroskopie und CMC-Messung für SDS<sub>VWR,23</sub> und SDS<sub>TS</sub> untersucht. Leider standen keine SDS<sub>VWR,21</sub>-Proben zur Analyse zur Verfügung. Der Einfluss der SDS-Qualität auf die Membranleistung wurde durch Filtrationsexperimente untersucht, bei denen ölfreie SDS-Lösungen und SDS-modifizierte emulgierte Öle durch zwei Arten von Kapillarmembranen verschiedener Hersteller filtriert wurden. Diese Versuche zeigten, dass die SDS-unterstützte Dead-End-UF-Methode empfindlich auf geringfügige Änderungen der Qualität des verwendeten SDS stark reagierte, wobei die Effizienz der BW bei Verwendung von SDS<sub>VWR,23</sub> und SDS<sub>TS</sub> stark verringert wurde.
  - d. Unsere Experimente zur Optimierung der Betriebsbedingungen, einschließlich Filtrationsfluss, Filtrationsdauer, BW-Fluss und BW-Dauer, führten nicht zu einer verbesserten Membranleistung. Dies kann auf den verwendeten SDS-Typ (d.h. SDS<sub>VWR,23</sub>) zurückgeführt werden, der sich als unwirksam bei der Wiederherstellung der Membranleistung durch BW erwies.
  - e. Ein höherer CO<sub>2</sub>-Fußabdruck wurde für die Tensid-unterstützte Dead-End-UF im Vergleich zum Cross-Flow-Betrieb berechnet. Die entwickelte Tensid-unterstützte Dead-End-UF erwies sich aufgrund der hohen Beschaffungskosten des SDS als weniger wirtschaftlich rentabel als der Cross-Flow-Betriebsmodus.
3. Das Projekt umfasste auch Untersuchungen zur Anwendbarkeit von Hybrid-UF-Prozessen, kombiniert mit PAC oder Koagulation: PAC-UF, Koagulation-UF und



PAC-Koagulation-UF. Es wurden Adsorptionsexperimente mit kommerziellen PAC-Produkten zur Untersuchung der Adsorptionsisothermen und Kinetik, Labor-Koagulationsexperimente (Jar-Tests) mit verschiedenen kommerziellen Eisen- und Aluminium-basierten Koagulantien und Filtrationstests zur Bewertung der Effizienz der Hybrid-UF-Prozesse durchgeführt.

- Ein erheblicher Teil der Ölkomponenten aus den emulgierten Ölen wurde auf dem PAC adsorbiert (bis zu 80%), ein gewisser nicht-adsorbierbarer Teil konnte jedoch festgestellt werden. Die Adsorption folgt höchstwahrscheinlich einer Mehrkomponenten-Adsorptionsisotherme. Die Adsorptionsisotherme konnte jedoch nicht bestimmt werden. Während der Adsorptionsisotherm-Experimente konnte eine hohe Schwankung der Eliminationsrate beobachtet werden. Adsorbierbare Komponenten wurden vermutlich an der äußeren Oberfläche der PAC-Partikel adsorbiert. Es konnten keine signifikanten Unterschiede bei der Verwendung verschiedener PAC-Typen festgestellt werden. Ein Adsorption-Gleichgewicht konnte nach 24 Stunden beobachtet werden.
- Die Dosierung von Eisen- und Aluminium-basierten Koagulantien verbesserte die Öleliminierung aus den Emulsionen, was hauptsächlich auf eine Erhöhung der Ölkoaleszenz zwischen den Öltröpfchen zurückzuführen ist. Eisenbasierte Koagulantien zeigten höhere Eliminationsraten als die auf Aluminium basierenden.
- Die Dosierung von PAC vor UF-Membranen reduzierte das Fouling nicht signifikant und verbesserte die Rückspüeffizienz nicht. Die Dosierung von Koagulantien vor UF-Membranen reduzierte die Fouling-Rate, verbesserte jedoch nicht die Rückspüeffizienz. Die Dosierung sowohl von PAC als auch von Koagulantien vor UF reduzierte das Fouling, konnte jedoch die Koagulation-UF-Operation nicht übertreffen.
- Die Dosierung von PAC verbesserte die Trennleistung der Membran im Vergleich zur alleinstehenden UF-Membran geringfügig, während die Dosierung von Koagulantien allein oder in Kombination mit PAC vor UF eine bessere Trennleistung zeigte.



4. Das Projekt umfasste auch praxisrelevante Experimente zur Untersuchung der Skalierbarkeit der Ergebnisse auf längeren Membranmodulen (1,4 m) mit einer vergrößerten aktiven Oberfläche (bis zu 0,23 m<sup>2</sup>). Diese Experimente umfassten langfristige Versuche von bis zu sechs Tagen. Die Dosierung eines eisenbasierten Koagulants in einer Konzentration von 1 mg/L vor der UF verbesserte die Membranleistung signifikant und reduzierte die Fouling-Rate, sodass die Filtration bis zu 80 Stunden ohne chemische Reinigung fortgesetzt werden konnte. Im Gegensatz dazu konnte die alleinstehende UF unter ähnlichen Bedingungen nur weniger als drei Stunden betrieben werden.

### 1.3 Fortschritte und Änderungen des ursprünglichen Zeitplans

Insgesamt wurden die geplanten Untersuchungen im Wesentlichen wie ursprünglich geplant durchgeführt. Allerdings waren einige Anpassungen notwendig. Änderungen am Plan oder Budget wurden ordnungsgemäß im Voraus bei der Willy-Hager-Stiftung beantragt und genehmigt, und alle Abweichungen wurden umfassend berichtet. Tabelle 1 bietet einen detaillierten Vergleich zwischen den geplanten Arbeiten und den tatsächlich im Projekt durchgeführten Arbeiten. Der Fortschritt kann wie folgt zusammengefasst werden:

- Zu Beginn des Projekts wurden zusätzliche ungeplante Arbeiten durchgeführt. Diese umfassten die Analyse der Mechanismen, die der verbesserten Leistung und der erhöhten Rückspüreffizienz durch den SDS-verbesserten UF-Prozess zugrunde liegen. Zusätzliche Anstrengungen wurden auch in die Durchführung weiterer Experimente, Analysen und die Modellierung der im W-UFO II Teilprojekt gewonnenen Ergebnisse investiert. Diese Arbeiten waren notwendig für die Vorbereitung eines Manuskripts für einen peer-reviewed Artikel, der erfolgreich im Journal Separation and Purification Technology veröffentlicht wurde.
- WP1: Die Arbeiten begannen wie geplant. Jedes Experiment sollte dreimal bei drei Ölkonzentrationen von 10, 25 und 50 mg/L durchgeführt werden. Nachdem die Experimente mit 25 und 50 mg/L, was zwei Dritteln der Experimente entspricht, abgeschlossen waren, wurde festgestellt, dass die gelöste Ölfraction nicht zu einer signifikanten Fouling führte. Folglich konnten Fouling-Mechanismen nicht

modelliert werden. Die Experimente mit einer Ölkonzentration von 10 mg/L wurden als unnötig erachtet, da kein Effekt der gelösten Ölfraction nachgewiesen werden konnte. Daher war die Anzahl der in WP1 durchgeführten Experimente geringer als ursprünglich vorgeschlagen. Die Zeit für diese Experimente wurde in andere Arbeitspakete investiert.

- In WP2 wurde Aufgabe (a) wie geplant durchgeführt. Die erzielten Ergebnisse waren sehr interessant und vielversprechend, sodass die Arbeiten an einigen Stellen erweitert wurden. In Unteraufgabe i wurden mehr Experimente durchgeführt, um zu untersuchen, ob der Aktivierungszustand des Pulveraktivkohles die Leistung des PAC beeinflusst. In Unteraufgabe iii wurde die doppelte Anzahl geplanter Experimente durchgeführt, weil es sehr interessant war, die erzielten Ergebnisse mit Membranen mit größerer Porengröße, d.h. MF-Membranen, zu vergleichen. Auch in Unteraufgabe iv wurden mehr Experimente durchgeführt. Hier wurden nicht nur Experimente mit einem PAC durchgeführt, sondern mit drei verschiedenen PAC-Typen und einigen Experimenten mit unterschiedlicher PAC-Dosierung.
- Während der Durchführung der Aufgaben (b) und (c) von WP2 wurde beobachtet, dass sich das Filtrationsverhalten der SDS-modifizierten emulgierten Öle von dem im W-UFO II Projekt unterschied. Diese Diskrepanz wurde zunächst auf potenzielle Variationen in der Qualität des von verschiedenen Lieferanten bezogenen SDS oder auf Änderungen der Membraneigenschaften zurückgeführt. Nach einer umfangreichen Untersuchung wurde festgestellt, dass die SDS-verbesserte UF-Methode empfindlich auf geringfügige Änderungen in der SDS-Qualität. Folglich wurden über 100 Experimente für diese Aufgaben durchgeführt, was die ursprünglich geplanten 70 Experimente überstieg. Aufgabe (c) war ursprünglich so konzipiert, dass sie einem statistischen Versuchsplan folgte; jedoch machten diese unvorhergesehenen erheblichen Schwankungen in den Materialien und die damit verbundenen Leistungsvariationen eine Anpassung und Erweiterung des Plans notwendig. Wir beschlossen, die Entwicklung mathematischer Beziehungen durch statistisches experimentelles Design auszusetzen und stattdessen mehr einzelne Experimente mit direkten Parametervergleichen durchzuführen, um Trends zuverlässig zu erfassen.

- In WP3 wurden die Aufgaben (a) und (b) wie geplant durchgeführt. Die vier für Aufgabe (c) geplanten Experimente konnten jedoch nicht abgeschlossen werden, da sie von den Ergebnissen der Experimente aus WP2(c) abhingen.
- In WP4 wurden die Kosten- und Umweltbewertungen sowie die Studie zu den Entsorgungsrichtlinien wie geplant durchgeführt
- In WP5 wurden die Langzeitexperimente mit Modulen in technischer Länge teilweise wie geplant abgeschlossen. Allerdings wurden die Experimente mit SDS-verbesserter UF nicht vollständig durchgeführt.

Insgesamt wurden mehr als 300 Experimente durchgeführt, im Vergleich zu den 269 im Projektantrag geplanten Experimenten.

**Tabelle 1: Eine detaillierte Liste der geplanten und durchgeführten Experimente in allen Arbeitspaketen während W-UFO III<sup>+</sup>**

WP	Task	Sub-Task	Pg*	Proposed experiments	Qty of Exp.	
					Plan	Done
1	a		18	Separation of model feed water at 3 oil concentrations (10, 25, 50 mg/L) using three filters (0.1, 0.2 and 0.45 $\mu\text{m}$ ) $\times$ 2 trials - analysis of permeates (TOC, oil droplet size distribution, WSO) and comparison with unfiltered model feed water.	18 + 63	12 + ~40
	b		18	One-cycle filtration experiments using 2 types of feeds (i.e., one filtered, and one unfiltered) $\times$ 3 oil concentrations (10, 25, 50 mg/L) $\times$ 2 trials	12	8
	c+ d		19	Modeling of fouling mechanisms and correlating between fouling mechanism and feed components for the outcome results from experiments of task (b)	12	-
2	a	i	19	Bench-scale adsorption experiments: adsorption isotherm experiments using 3 types of PAC at 50 mg/L and oil concentration of 25 mg/L, 2 trials. Adsorption kinetics experiments using three PAC concentrations and oil concentrations of 25 mg/L, 2 trials	24	28
		ii	19	Lab-scale coagulation tests: 2 types of coagulants (one Fe-based and one Al-based) $\times$ 3 - 5 different dosages $\times$ 1 oil concentrations (25 mg/L) $\times$ 2 trials	20	20
	iii	20	One filtration-cycle experiments using 5 permeates (i.e., three from PAC process and two from coagulation process) $\times$ 1 oil concentrations (25 mg/L) $\times$ 2 trials	10	20	
	iv	20	Lab-scale hybrid experiments using 3 combinations (PAC-UF, coagulant-UF, PAC-coagulant-UF) (one PAC type and one coagulant type) $\times$ 1 oil concentration (25 mg/L) $\times$ 2 trials	6	16	
	b+c	-	20	Mini plant tests: <ul style="list-style-type: none"> <li>• Dead-end: 3 SDS dosing scenarios (i.e., one-time, continuous, periodic dosing) <math>\times</math> 1 oil concentrations (25 mg/L) <math>\times</math> 2 trials</li> <li>• Crossflow: 2 CFV (0.75, 2.5 m/s) <math>\times</math> 1 oil concentrations (25 mg/L) <math>\times</math> 2 trials</li> <li>• Optimizing operation conditions: Flux, Duration, BW Flux, BW Duration and pure water duration after BW</li> </ul>	~70	105
3	a		23	Reproduction of synthetic oily feed from literature at two oil concentrations (10, 25 mg/L), characterizations (oil droplet size distribution, TOC, WSF), 2 trials	12	~12
	b		24	Lab-scale dead-end and crossflow filtration experiments without SDS dosing: 3 filtration conditions (i.e., dead-end, crossflow@ CFV 0.75 and 2.5 m/s) $\times$ 2 oil concentrations (10, 25 mg/L) $\times$ 2 trials.	12	12
	c		24	Lab-scale dead-end filtration experiments with SDS dosing @optimized conditions $\times$ 2 oil concentrations (10, 25 mg/L) $\times$ 2 trials.	4	0

WP	Task	Sub-Task	Pg*	Proposed experiments	Qty of Exp.	
					Plan	Done
5	a		24	Long term dead-end and crossflow (using one CFV) filtration experiments, one oil concentration 25 mg/L, constant operation period (7 days), 2 trials	4	2
	b		24	Long term combined PAC / coagulation with SDS-enhanced UF filtration experiments in dead-end operation, one oil concentration 25 mg/L, constant operation period (7 days), 2 trials	2	1
Subtotal					269	273
Additional Experiments				With membrane from different supplier	-	8
				With SDS from different supplier	-	8
				SDS quantification method	-	12
Total Sum					269	301

\* Page number in the W-UFO III+ Proposal

## 1.4 Veröffentlichungen

Während des W-UFO III+ wurden die wichtigsten wissenschaftlichen Ergebnisse des W-UFO-Projekts in zwei peer-reviewed Papers, zwei Konferenzpapieren, vier nationalen und internationalen wissenschaftlichen Konferenzen Vorträge und drei als Posters wie folgt vorgestellt:

Folgende peer-reviewed Papers wurden veröffentlicht:

1. Idrees, H., Al-Ethawi, A., ElSherbiny, I. M. A. and Panglisch, S. 2023. Surfactant-enhanced dead-end ultrafiltration for tertiary treatment of produced water. Separation and purification technology, 311, 123225.
2. Idrees, H., Alhanini, H., Panglisch, S. & Elsherbiny, I. M. A. 2024. Assessment and Upgrading of Preparation Protocols for Emulsified Crude Oils Mimicking Real Produced Water Characteristics Chemie Ingenieur Technik, 96, 513-521.

Folgende Konferenzpapiere wurden veröffentlicht:

1. Idrees, H., ElSherbiny, I. M. A., & Panglisch, S. (2023). Promoting organic fouling reversibility via introduction of sodium dodecyl sulfate prior to ultrafiltration of produced water, in IWA Particle Separation 2023, Johannesburg – South Africa.
2. Idrees, H., ElSherbiny, I. M. A., & Panglisch, S. (2023). Promoting fouling reversibility via introduction of sodium dodecyl sulfate prior to ultrafiltration of produced water in polishing step. In Filtech 2023, Cologne - Germany.

Die Arbeit wurde auf folgenden Konferenzen als Vorträge vorgestellt:

1. IWA Particle Separation Conference, Dezember 2023, Johannesburg, Südafrika
2. DAAD Knowledge Exchange Workshop, Oktober 2023, Alexandria, Ägypten
3. Filtech, Februar 2023, Köln
4. Achema Congress, August 2022, Frankfurt

Die Arbeit wurde auf folgenden Konferenzen als Posters vorgestellt:

1. Jahrestreffen der DECHEMA/VDI-Fachgruppe Membrantechnik, Februar 2024, Frankfurt
2. MemDes, 6<sup>th</sup> International Conference on Desalination using Membrane Technology, November 2023, Sitges, Spanien
3. Aachener Membran Kolloquium, 2022, Aachen

Drei zusätzliche Manuskripte werden nach Abschluss des Projekts eingereicht:

- „Einsatz von Membrantechnologie zur effizienten Aufbereitung ölhaltiger Abwässer“ wird Anfang August für “Wasser und Abfall” Journal eingereicht.
- “Influence of oil droplet size distribution on the fouling mechanisms of UF/MF membranes during filtration of oil emulsions”. Ursprünglich geplant für das Journal

„Desalination“, das Journal könnte jedoch noch geändert werden. Der Abgabetermin ist noch nicht festgelegt.

- “Enhanced dead-end ultrafiltration via combination with PACs and coagulant for tertiary treatment of produced water”. Journal wird später festgelegt

## 2 Summary of the main scientific outputs

### 2.1 Literature review

A comprehensive literature review was conducted to address several pertinent topics. Initially, the methods employed in existing literature for producing synthetic emulsified oil were examined. This examination was essential to ensure the applicability of the acquired results when filtering emulsions prepared using different methodologies. Subsequently, the discharge regulations for oily produced water and potential reuse applications were reviewed across various relevant regions and countries. Further literature was also reviewed regarding the enhancement of membrane performance through surfactant dosing and the hybrid operation of powdered activated carbon (PAC) and/or coagulation with ultrafiltration (UF). Additionally, references related to the environmental impact of the developed surfactant-enhanced dead-end UF method were investigated.

#### 2.1.1 Protocols for the production of synthetic oily wastewater effluents

Various emulsification techniques are employed in literature [1-3]. Tadros et al. (2016) found that high-pressure homogenization (HPH) and ultrasonication (US) produced smaller droplets compared to stator-rotor mixers and colloid mills [1, 4-6]. Prof. Czermak's research found HPH most suitable for tertiary produced water (PW) treatment [2], with Ebrahimi et al. (2018) using HPH to simulate real PW samples [4]. They produced emulsified oils with droplet sizes from 0.1 to 20  $\mu\text{m}$ , peaking at 1.8  $\mu\text{m}$ , and maintaining stability for up to ten days. Dardor et al. (2021) used ultrasonication to replicate PW characteristics, achieving stability over 80 days with droplet sizes from 1  $\mu\text{m}$  to 63  $\mu\text{m}$  [7]. Another group used sonication for 6 hours to produce synthetic PW, suitable for low-volume experiments [8, 9].

#### 2.1.2 Management of produced water

When planning an offshore project, regulatory bodies conduct environmental impact assessments to evaluate potential impacts on the environment and marine ecosystems.



Developed in Norway, the environmental impact factor considers various factors of PW discharge [10].

Management of PW effluents vary based on composition, reinjection needs, and local regulations. Advanced countries typically use two monitoring techniques: one for discharge quality and another for environmental impacts on marine life. However, many developing economies lack sufficient or enforced regulations to prevent water contamination [11, 12].

### ***2.1.2.1 Discharge methods and their limitations***

Produced water treatment varies between onshore and offshore facilities due to space, weight restrictions, and differing treatment priorities. Onshore facilities focus on reducing salt content, while offshore facilities prioritize meeting oil and grease discharge limits [13]. Offshore PW is discharged into oceans after treatment, following environmental regulations [14, 15]. High Total Oil and Grease (TOG) concentrations can negatively impact ecosystems by coating plants and animals, leading to oxygen depletion and suffocation. Discharge limits for TOG concentrations vary globally, highlighting the importance of adhering to regional guidelines to mitigate environmental impacts [16].

#### ***a. Germany and OSPAR conviction***

Countries including Germany, Belgium, Netherlands, France, Spain, Portugal, Finland, Sweden, Ireland, Switzerland, Denmark, Norway, Iceland, Luxembourg, and the United Kingdom follow OSPAR<sup>1</sup> limitations for offshore facilities [10]. The OSPAR Commission, established in 1998, merged and updated the OSPAR to regulate marine waste disposal and pollution. OSPAR follows two main principles: the precautionary principle and the polluter-pays principle, aiming to minimize hazardous discharges [10, 12, 17].

In 2001, OSPAR set an initial offshore oil discharge limit at 40 mg/L TOG, reducing it to a monthly average of 30 mg/L by 2006. Between 2009 and 2019, discharge concentrations averaged between 12.4 to 14.1 mg/L, well below the limit. The North-East Atlantic

---

<sup>1</sup> Convention for the Protection of the Marine Environment of the North-East Atlantic

Environment Strategy (NEAES) 2010-2020 strategy addressed climate change, ocean acidification, and eutrophication, with further updates in NEAES 2030 [14, 17, 18].

The OSPAR Offshore industry committee and hazardous substances and eutrophication committee oversee oil and gas industry spills, discharges, and emissions, identifying contaminants affecting the marine environment. OSPAR prohibits the dumping or abandonment of unused oil and gas infrastructure, requiring decommissioned structures to be disposed of onshore [19].

### ***b. USA***

In the USA, about 47% of onshore PW is disposed of via deep injection wells, 46% is reused in oil or gas extraction, 3% is discharged into the environment, less than 1% is treated for beneficial reuse, and 3% is lost to evaporation [13, 20]. Over 80% of offshore PW is discharged into the ocean, following TOG limits determined by United States Environmental Protection Agency (EPA) [13]. PW management is governed by a complex framework of federal, state, and local regulations, primarily overseen by the EPA. The Clean Water Act's National Pollutant Discharge Elimination System and the Safe Drinking Water Act's Underground Injection Control program regulate surface discharge and deep well injection, respectively. States west of the 98th meridian have different discharge limitations compared to eastern states. Offshore facilities follow effluent guidelines with TOG limits set at 29 mg/L monthly and 42 mg/L daily [15, 20, 21].

### ***c. Africa***

Nigeria, the sixth largest oil producer globally and the largest in Africa, has seen significant environmental degradation in the Niger Delta due to oil spills and improper PW discharge. Regulations and monitored parameters are often not strictly applied, and the guidelines are not diverse enough to ensure non-hazardous discharges [22, 23]. The Department of Petroleum Resources regulates PW discharges through the Environmental Guidelines and Standards for the Petroleum Industry in Nigeria. It limits onshore TOG discharge to 10 mg/L and coastal and offshore discharge to 20 mg/L, but these guidelines are less stringent compared to international standards [22, 24, 25].

### **2.1.2.2 Reuse applications and their limitations**

With stringent discharge standards, there is increasing research and adoption of PW recycling processes. If treated to meet required standards, PW can become a valuable resource [15]. Treatment typically involves removing insoluble oil, boron, iron, and microorganisms, followed by specific treatments based on reuse needs [26]. Common PW reuse techniques include reinjection, agricultural irrigation, consumption by livestock, and use in industrial processes and cooling systems [14, 15, 27]. Reusing PW aids in disposal and enhances oil recovery [14, 15, 27]. Internal reuse within the oil and gas industry, such as PW reinjection, is cost-effective and widely practiced, with over 90% of PW reinjected globally to maintain hydraulic pressure and improve recovery. Reinjection regulations require TSS levels below 10 mg/L and TOG concentrations under 42 mg/L [14]. Hydraulic fracturing also uses PW, especially in water-scarce regions like the Permian Basin in Texas. Excess PW, after treatment, is injected into deep wells, though high reinjection rates can induce seismic activity [28, 29]. While treating PW to drinking water standards is costly and generates saline brine, PW can be used for agricultural irrigation, livestock, and wildlife if treated for salinity and toxicity [27, 29]. Additionally, PW can serve industrial purposes, firefighting, dust control, and equipment washing, provided it meets discharge standards to prevent environmental harm [14, 29].

### **2.1.3 Environmental and economic assessment**

To assess the feasibility of new strategies for PW treatment, they were compared to the crossflow operation standard, focusing on dosed substances, electrical energy consumption, and membrane replacement frequency. Long-term data on membrane lifetime were unavailable, so the study prioritized environmental and economic feasibility. The Carbon Footprint (CFP) is a key measure of environmental sustainability, reflecting carbon emissions from specific activities. CFP, originally part of the "ecological footprint" concept, has evolved to measure carbon emissions in mass rather than land area, gaining popularity among various stakeholders despite confusion over its definition [30, 31]. Global Warming Potential is used to assess greenhouse gases emissions over a 100-year period [32]. The Carbon Intensity (CI) of economic activities, like electricity generation, has decreased in Europe due to renewable energy adoption [33-35]. Different products have varying CFP values based on production methods. Surfactants like SDS, classified as emerging

contaminants, pose environmental risks due to improper disposal, with limited regulation. A study on Sodium Lauryl Ether Sulfate estimated a CFP of 1,870 kg CO<sub>2</sub>e per ton [36]. The CFP of electricity varies by country, with European countries generally showing a decrease in CI over time due to renewable energy adoption [37].

## 2.2 Materials and Methods

### 2.2.1 Chemicals

For the preparation of emulsified oils, a light standard crude oil (AR-2048, 2.01 wt.% Sulfur), from Alpha Resources LLC, USA, was used. In this study, three SDS products SDS<sub>VWR21</sub> (procured from VWR international, Belgium in 2021), SDS<sub>VWR,23</sub> (procured from VWR international, Belgium in 2023) and SDS<sub>TS</sub> (procured from Thermo Scientific, India) were used. Unless otherwise specified, all experiments in this study were conducted using SDS<sub>VWR,21</sub>. Coagulants Nüscofloc Fe and Nüscofloc ALF were provided by Dr. Nüsken Chemie GmbH, Germany. PAC adsorbents were made by milling three commercially available granular activated carbon products, ABG-H, HMA-B and ORG-K, made from the different raw materials wood, anthracite, and coconut shells, respectively.

### 2.2.2 Membranes

A set of MF and UF polyether sulfone (PES) flat sheet membranes with different average pore diameters were employed, see Table 1. All membrane samples had an active surface area of 13.85 cm<sup>2</sup>.

**Table 1: Specifications for flat sheet membranes employed in this project**

Acronym	Commercial name	Average pore diameter or MWCO	Produced by
UP150	Nadir <sup>®</sup> UP150	150 kDa	Mann+Hummel
S450	Supor <sup>®</sup> 450	0.45 μm	Pall
S200	Supor <sup>®</sup> 200	0.20 μm	Pall
S100	Supor <sup>®</sup> 100	0.10 μm	Pall

Two types of capillary membranes were implemented, Multibore membrane modules from Inge-Dupont GmbH, Germany and X-Flow from Pentair, Germany. Both membranes exhibit a nominal pore diameter of 20 nm. These membranes were implemented at different module configurations, as indicated in Table 2. The main difference between the modules was the total surface area.

**Table 2: Specifications for capillary membrane modules employed in this project**

Acronym	Active Surface area cm <sup>2</sup>	Module type	Nr. of capillaries	Membrane type
SM	515	Short (Rx)	70 (10 Fibers)	Multibore
SM <sub>1</sub>	51.5	Short (Rx)	7 (1 Fiber)	Multibore
LM	0.22	Long	8	Multibore
LM <sub>2</sub>	0.055	Long	2	Multibore
SX	800	Short (Rx)	12	X-Flow

### 2.2.3 Preparation of emulsified oil

The crude oil was mixed with pure water at volumetric ratio of 1:250 (oil/water) using a high-speed stator-rotor mixer (Ultra-Turrax® T 25, IKA, Germany) to prepare the premix emulsion. A high-pressure homogenizer (HPH 2000/4-SH5, IKA, Germany) was then applied to the premix twice at a pressure of 1,000 bar to produce the emulsified oil. To mimic a treated PW stream after primary and secondary treatments, the emulsified oil was filtered using a qualitative filter paper grade 310 with a particle retention of 13 µm (VWR, Germany) to remove micro-sized oil droplets with sizes > 10 µm. Thereafter, the stock emulsified oil was diluted using pure water to prepare emulsified oil batches with different oil concentrations in range of 5 - 50 mg/L as TOC (Shimadzu TOC-L, Japan). For surfactant-modified emulsified oil, SDS was dosed below the critical micelle concentration (CMC) at different concentrations in range of 0.024 - 1.2 g/L that are equivalent to 0.01 – 0.5 x CMC; 1 x CMC of SDS is equivalent to 2.4 g/L (8.2 mmol/L) at a temperature of 25 °C.

### 2.2.4 Characterization of the emulsified oils

#### 2.2.4.1 Determination of WSO fraction

The WSO fraction in the prepared emulsified oils was separated to examine its influence on membrane fouling (cf. section 2.3.2.2). Three methods were tested. The first method was based on the quantification of PAHs following the DIN 38407–39:2011–09 using gas chromatography with a mass spectrometric detector (GC–MS, model 5973, Hewlett-Packard, USA). This analysis was made at GBA Gesellschaft für Bioanalytik mbH, Germany. The two other methods were tested using GC-MS (see section 3.4.1.1 in the final W-UFO report) and Fluorophotometer with emission-excitation matrix (FEEM; see section 3.4.1.2 in the final W-UFO report) in our labs at the university of Duisburg-Essen.

### **2.2.4.2 Quantification of the SDS concentration**

The SDS concentration in the emulsified oil was analyzed using four methods, cf. section 3.4.2 in the final W-UFO report. The first method measured TOC content with a TOC-L device (Shmidazu, Japan). The second method used ion chromatography (Metrohm Ltd, Switzerland) as reported in literature. The third method utilized electrical conductivity (Cond-197i, WTW Instruments, Germany) with a calibration curve for SDS from 0 to 4.8 g/L. The fourth method was the Stains-all dye method. This involved preparing a working solution, maintaining pH with a Sorensen phosphate buffer, and measuring samples with a UV-Vis spectrophotometer (Lambda 20, PerkinElmer, Germany) at 220–600 nm.

### **2.2.4.3 Quality analysis of SDS samples**

The quality of both SDS<sub>TS</sub> and SDS<sub>VWR,23</sub> was analyzed. An elemental analysis was conducted to determine the carbon, hydrogen, nitrogen, and sulfur content. This analysis was performed by the Microanalytical Laboratory at the Faculty of Chemistry, Institute of Inorganic Chemistry, University of Duisburg-Essen. Three samples of each type of SDS were analyzed. Fourier transform infrared (FT-IR) was also analyzed using an FT-IR spectrometer from PerkinElmer, Germany. The CMC value was also experimentally measured, alongside two reference SDS samples with purities of 95% and >99%. These measurements were conducted at the labs of MSB Breitwieser MessSysteme, Augsburg, Germany.

### **2.2.5 Adsorption experiments**

To investigate adsorption behavior, experiments were conducted using three PAC products milled from granular activated carbon products (ABG-H, HMA-B, and ORG-K) made from wood, anthracite, and coconut shells. Kinetic tests with PAC dosed at 50 mg/L in emulsified oil (25 mg/L) were sampled over 48 hours. Adsorption isotherms were created by varying PAC concentration (1–400 mg/L) in emulsified oil, with samples analyzed for Ultraviolet spectral absorption coefficient at wavelength of 254 nm (UV<sub>254</sub>) and dissolved organic carbon (DOC).

## 2.2.6 Coagulation/flocculation jar-test experiments

To optimize coagulation/flocculation for oil removal, jar tests were conducted using iron- and aluminum-based coagulants at 0-12 mg/L and 0-6 mg/L, respectively, following the W218 DVGW protocol. The 1.8 L oil emulsion (25 mg/L) was mixed in 2 L beakers. Samples were taken and analyzed for DOC, UV<sub>254</sub>, turbidity, pH, and conductivity after pH adjustment to ~7.0.

## 2.2.7 Dead-end filtration experiments

Multiple-cycle dead-end filtration experiments with periodic hydraulic backwashing were conducted at constant flow rate employing a fully automated mini-plants membrane testing unit (convergence B.V., Netherlands). Unless else specified, a mini-plant testing experiment was started by filtering pure water at flux of 100 L/(m<sup>2</sup>·h) for 15 min to determine initial pure water permeability. Thereafter, multiple filtration cycles were conducted at constant flux of 100 L/(m<sup>2</sup>·h). Every filtration cycle lasted for 45 min, then it was followed by a hydraulic backwashing at a flux of 230 L/(m<sup>2</sup>·h) for 90 s. The alterations in transmembrane pressure were recorded through different testing steps, and normalized permeability decline was calculated. In case of severe membrane fouling, experiment was automatically aborted when the transmembrane pressure reached the maximum value set at 4 bar.

## 2.2.8 Hybrid UF tests with the dosage of PAC and/or coagulants

Hybrid filtration experiments tested coagulation-UF, PAC-UF, and coagulation-PAC-UF combinations. Standalone membrane filtration was first performed on surfactant-free emulsified oils (10 and 25 mg/L) using S100 and UP 150 flat sheet membranes. In coagulation-based tests, coagulant was added and mixed rapidly, then slowly. PAC-based tests formed a PAC cake layer on the membrane before filtering emulsified oil. All experiments measured filtered volume per unit time to calculate permeability, and samples were analyzed for TOC, UV<sub>254</sub>, conductivity, pH, and turbidity. Capillary membrane modules (SM<sub>1</sub> and SM<sub>2</sub>) were also used with similar methods, including backwash steps to test efficiency.

## 2.2.9 Semi-technical length and long-term hybrid filtration experiments

To examine upscaling, lab-scale experiments used semi-technical membrane modules with active areas of 0.22 m<sup>2</sup> (LM) and 0.055 m<sup>2</sup> (LM<sub>2</sub>). Long-term tests employed the “SRA filtration plant,” operating at up to 60 L/h flow rate and 2.5 bars pressure. The unit features feed and backwash pumps, PID controllers, magnetic valves, and dosing pumps for coagulant and PAC.



## 2.2.10 Environmental and economic assessment

To evaluate the feasibility of the developed strategies, a comparison was made with the crossflow operation, which served as the reference. In this study, the focus was on examining the differences in dosed substances and electrical energy consumption. These differences formed the basis for assessing the environmental and economic feasibility of the enhanced dead-end methods. These parameters were presented and quantified in terms of cost and CFP. Refer to section 3.11 in the final W-UFO report for more details.

## 2.3 Results and discussion

### 2.3.1 Contribution of water-soluble oil fraction in the membrane fouling

Before optimizing the treatment process, it was important to effectively separate and quantify the WSO in the model feed water and in the permeate water. Two steps were carried out for this purpose: First, separation and quantitative determination of WSO, where separation was investigated with filtration of the model feed water through 0.2 and 0.45  $\mu\text{m}$  filters. Secondly, filtration tests with the permeates obtained to determine the contribution of WSO to membrane fouling.

In this project, two types of techniques were used to determine the dissolved oil fractions, one method using a fluorophotometer with emission excitation matrix, FEEM, according to the ASTM D5412-93 standard method, and another method using gas chromatography analysis performed in different ways.

Components of surfactant-free oil emulsions with oil concentration of 25 mg/L and the permeates of S450 and S200 membranes were analyzed with GC-MS and stir bar sorptive extraction using Gerstel-Twisters<sup>®</sup> as explained in section 3.4.1.1, in the final W-UFO report. Figure 1 shows the spectrum of surfactant-free oil emulsions with an oil concentration of 25 mg/L.

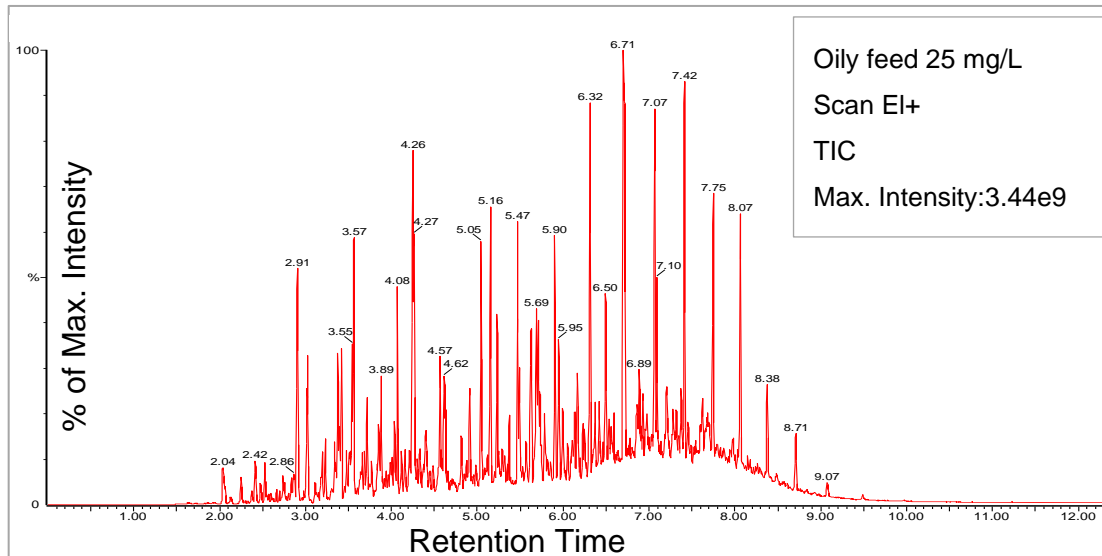


**Figure 1: GC-MS analysis of surfactant-free emulsified oily feed with oil concentration of 25 mg/L as TOC**

Further analysis of the chromatographic results included integrating the area of the main intensity peaks and a qualitative analysis by comparison with the NIST library. As indicated in Figure 2, components identified in the feed (among others) were methylcyclohexane, toluene, ethylbenzene, p-xylene, di-tert-butyl disulfide, methylnaphthalene, tetradecane, tetradecane, 2,6,10-trimethyl, pentadecane, 2,6,10,14-tetramethyl and nonadecan/heneicosane. They showed a statistical probability of 71%, 38%, 65%, 38%, 46%, 30%, 34%, 17%, 25% and 13%, respectively. These compounds were chosen as “reference compounds” for further analysis due to their clearly separated peaks, sufficient intensities and their different molecular properties. It should be noted that the qualitative identification of longer aliphatic chains is statistically more uncertain than that of smaller aromatics because the pattern of the MS-fragments is less clear. As these compounds appear later in the chromatogram, i.e. they have longer retention times than smaller aromatics, the statistical probability values

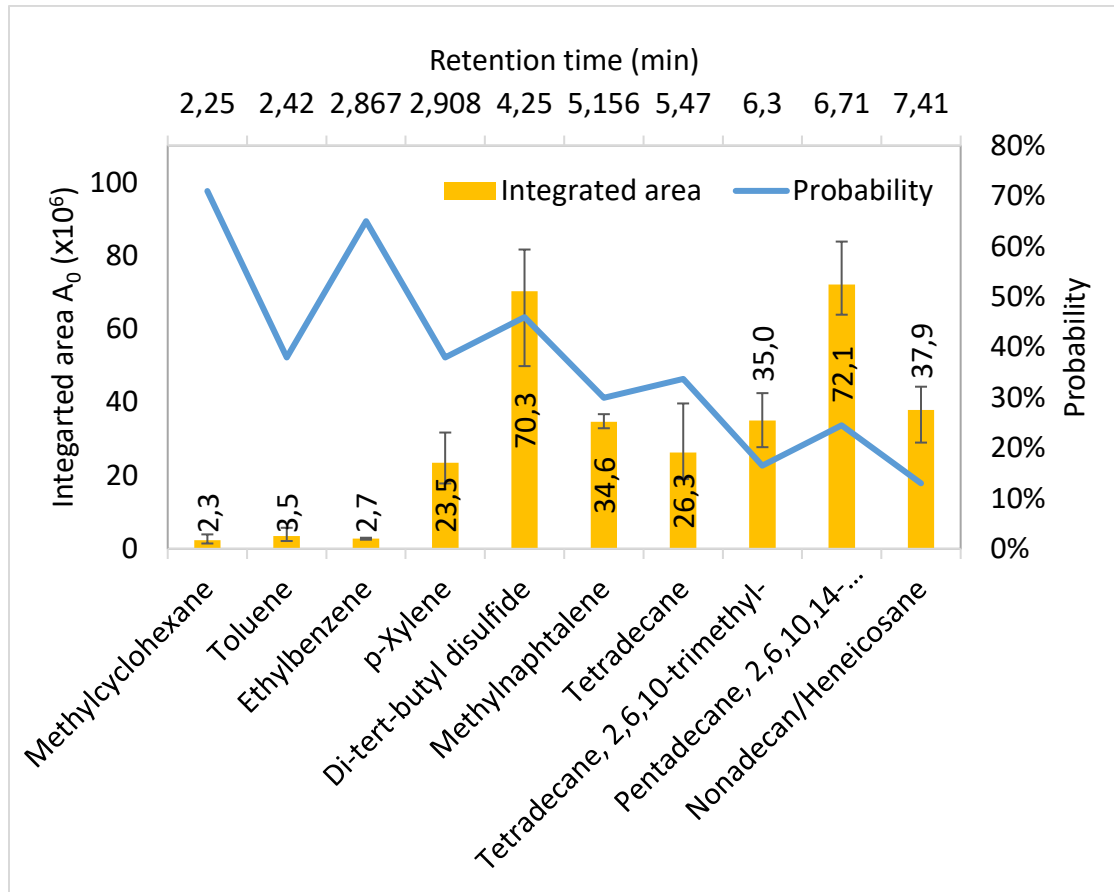


**Figure 2:** Reference components of surfactant-free emulsified oil that were detected with the GC-MS analysis with their respective retention time, integrated area of the intensity peak and probability of the detected component compared to the NIST library. Presented as average of four trials with the min. and max. error bars

Furthermore, Figure 3 shows the relative area  $A_i/A_0$  which is the ratio of integrated area of the respective peaks ( $A_i$ ) of the permeates of S450 and S200 membranes related to the integrated area of the reference intensity peak of the feed ( $A_0$ ). In which, it can be noticed that some components like tetradecane, tetradecane, 2,6,10-trimethyl, pentadecane, 2,6,10,14-tetramethyl and nonadecan/heneicosane were completely removed by both filter types. Other components, like di-tert-butyl disulfide, may penetrate the filters as they were detected in the permeate of both filters. Some components, like methylnaphthalene, were detected in the permeate of S450 with relative area about 30% of feed intensity but at low relative area <3% in permeate of S200. Other components like methylcyclohexane, toluene, ethylbenzene, p-xylene were detected in the permeate of both S450 and S200.

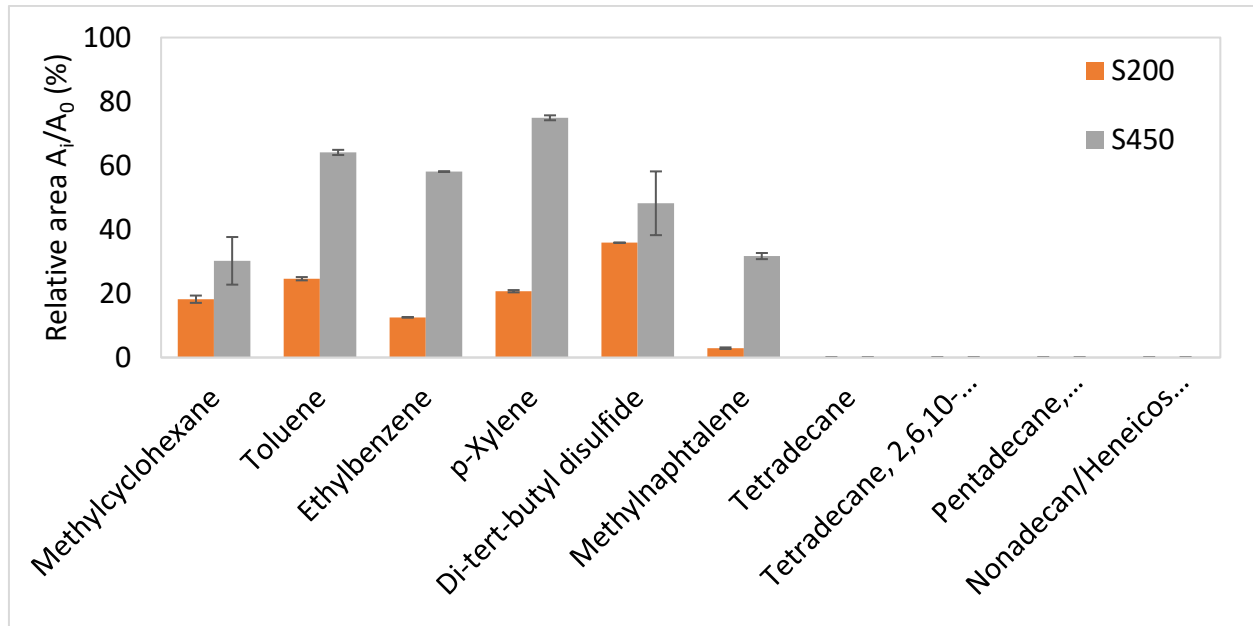


**Figure 3:** Relative area  $A_i/A_0$ , integrated area of intensity peaks ( $A_i$ ) of the reference components in the permeate of S450 and S200 membranes related to the respective integrated area of the intensity peak of the feed ( $A_0$ ). Presented as average of two trials with the min. and max. error bars

filtering the permeate of S450 through SM resulted in lower PAH concentrations in the permeate of the SM membrane as indicated in Figure 4.

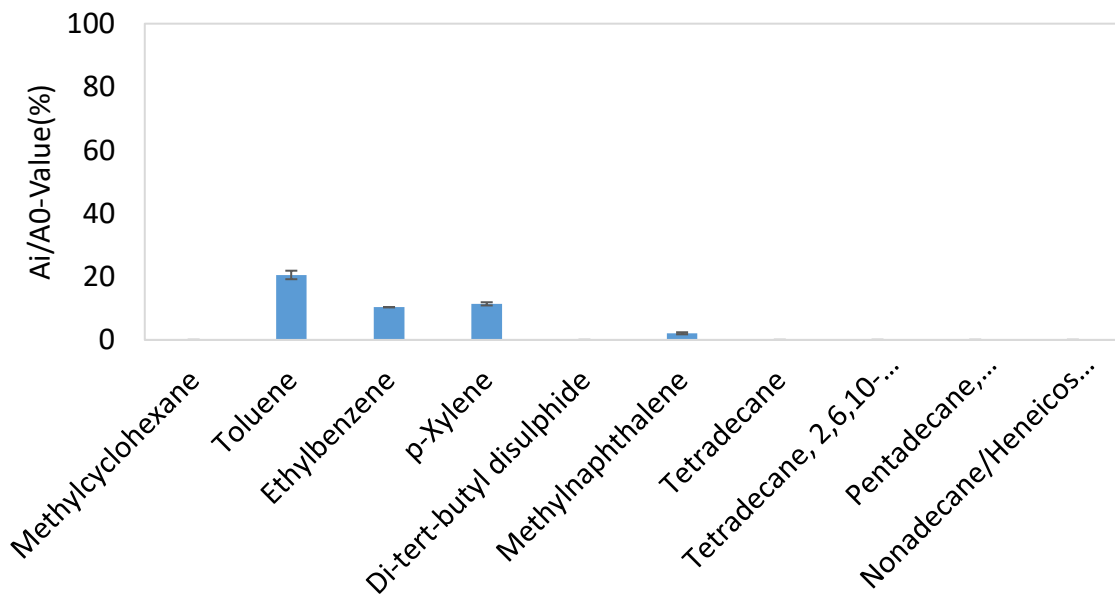


**Figure 4:** Relative area  $A_i/A_0$ , of the permeate of SM membranes, when filtering the permeates of S450 membranes through SM membrane.

Moreover, the permeates gained by the filtration using S450 and S200 membrane were filtered through SM<sub>1</sub> UF membrane module in single-cycle filtration experiments. Generally, much less performance decay was found compared to the treatment of emulsified oil, which may imply the role of the emulsified oil droplets (and coalescence) in the fouling mechanisms during filtration of surfactant-free emulsified oil. For instance, as indicated in Figure 5, treating the permeate of S450 by the UF membrane showed only a very low permeability decline from ~ 530 L/(m<sup>2</sup>·h·bar) to ~ 523 L/(m<sup>2</sup>·h·bar), i.e., the membrane lost only about 2 % of its initial permeability at the end of the filtration cycle.

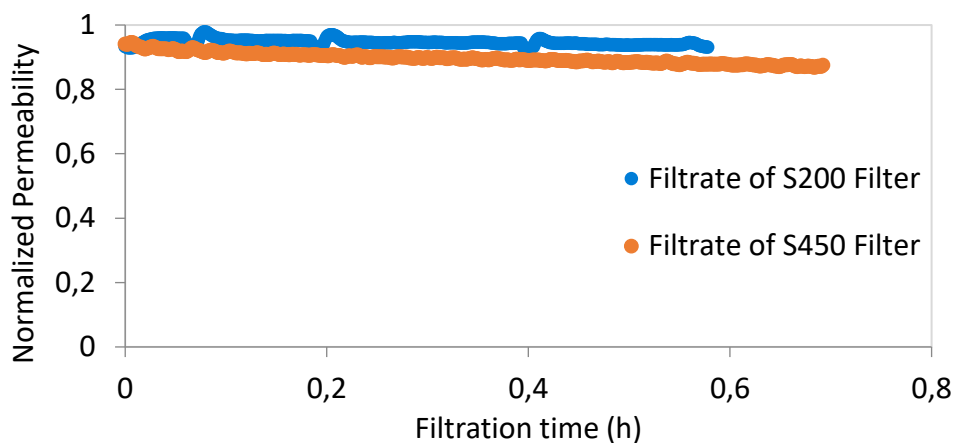


**Figure 5:** Normalized permeability of SM<sub>1</sub> membranes during single-cycle filtration experiment with the permeates of S100, S200 and S450 as feed

Furthermore, extending the cycle duration to 5h did not indicate a significant permeability decline. As it was shown in Figure 3, most of the dissolved oil fraction can pass through S450 this result emphasizes the finding that the dissolved oil fraction does not contribute significantly to membrane fouling.

## 2.3.2 Further investigations on the surfactant-enhanced dead-end UF

### 2.3.2.1 Understating the role of SDS in promoting membrane antifouling propensity in dead-end ultrafiltration of emulsified oils

Based on the knowledge gained, there are three proposed effects induced by SDS dosing prior to dead-end ultrafiltration of emulsified oils that are jointly responsible for the promoted hydraulic fouling reversibility and substantially improved mechanical backwashing efficiency, as illustrated in Figure 6.

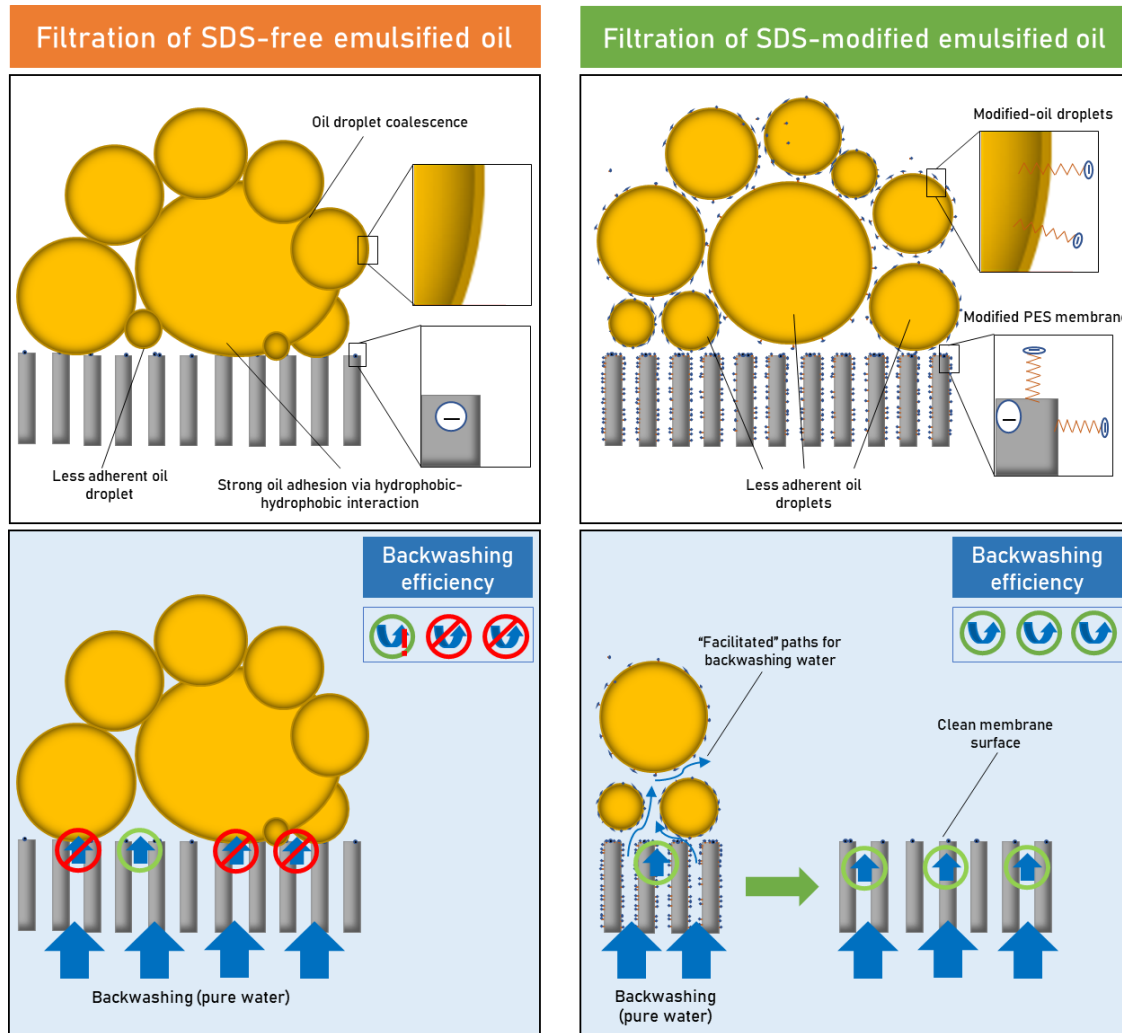


**Figure 6: Representation for the proposed joint effects induced by SDS dosing prior to ultrafiltration that are responsible for the substantially improved membrane antifouling performance vs. strong membrane fouling caused by dead-end ultrafiltration of SDS-free emulsified oil**

*(i) Modification of emulsified oil characteristics via the adsorption of SDS molecules at the oil/water interface:*

SDS-modified oil droplets exhibited an increased negative zeta-potential values compared to surfactant-free emulsified oil (See in Section 4.3.1.1 and Table 17 in the final W-UFO report). These negatively charged (or modified) oil droplets were found to be more stable and less susceptible to coalescence during membrane filtration (in the membrane vicinity). Moreover, they can be less adherent into the PES membrane matrix (that might be also

modified by SDS) because of less (or prohibited) hydrophobic-hydrophobic interaction. These findings are consistent with recent literature [38-41].

(ii) *Modification of membrane surface characteristics via the adsorption of SDS monomers:*

SDS monomers (below CMC) can be readily adsorbed into PES membrane matrix (cf. Section 4.3.1.2.1 in the final W-UFO report). Consequently, they modify membrane surface characteristics by inducing negative charges that can minimize hydrophobic-hydrophobic interactions with the emulsified oil, i.e., a surfactant coating to the membrane to mitigate oil adhesion. The reliability of precoating mechanism was separately examined as a possible standalone mechanism for the observed superior membrane performance as presented in Figure 7. Nevertheless, the results showed that it cannot be solely responsible for the promoted fouling reversibility in the SDS-enhanced ultrafiltration process.

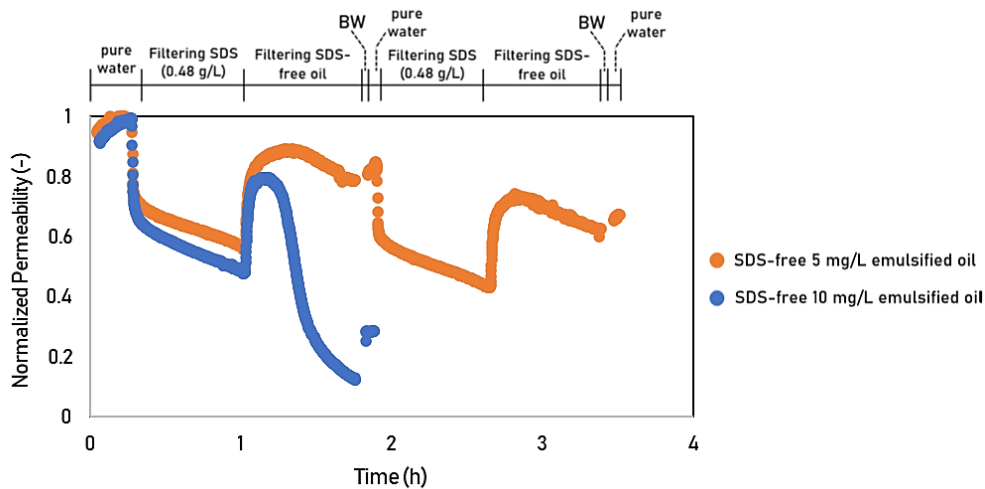


**Figure 7: Normalized permeability curves for specially designed multiple-cycle dead-end filtration tests, starting with filtration of 0.48 g/L oil-free SDS solution at a constant flux of 100 L/(m<sup>2</sup>·h) followed by filtration of surfactant-free emulsified oils (5 mg/L or 10 mg/L)**

(iii) *Promoting the access of backwashing water via the adsorbed SDS molecules in the formed fouling layer (both adsorbed to membrane surface and emulsified oil droplets):*

The adsorbed surfactant monomers in the composite fouling layer formed during the dead-end filtration of SDS-modified emulsified oils can decrease the interfacial surface tension between oil and water, offer “facilitated” paths for the backwashing water through the



fouling layer, and consequently, promote the backwashing efficiency. Such facilitated access of backwashing water into the oil fouling layer and the superior hydraulic backwashing efficiency were found to be achievable only through the filtration of SDS-modified emulsified oils, while sequential filtrations of surfactant and emulsified oil (and *vice versa*) caused significantly less hydraulic backwashing efficiency.

The three effects are believed to contribute into the observed superior performance by SDS-enhanced ultrafiltration process. Nevertheless, since mini-plant filtration experiments using SDS-modified 5 mg/L and 10 mg/L emulsified oils revealed that there is a minimum SDS dose that should be maintained to obtain the desired enhanced membrane performance (cf. Sections 4.3.1.4.1 and 4.3.1.4.2 in the final W-UFO report), one can conclude that modifications of emulsified oil droplets and the PES membrane by the SDS are the most influencing effects.

### **2.3.2.2 Quantitative determination of the SDS concentration in UF permeates**

One of the challenges was to determine the SDS concentration in the permeate of the UF membrane. Within this work, based on literature review, four methods were examined for the quantification of the SDS. TOC [42], ion chromatography [43], conductivity [44], and spectrophotometric analysis [45], cf. section 2.2.4.2. Although these methods were reported in the literature as successful ways for the SDS quantification, replicating them in our lab indicated some difficulties and drawbacks for each method (see section 4.3.1.6.3 in the final W-UFO report)

Due to the foam that is formed by SDS, TOC analysis was not accurate method for detecting the SDS content. The implemented ion chromatography method could not successfully detect the dodecyl sulfate and was significantly disturbed by the impurities present in the employed SDS.

The electrical conductivity method reported by [44] was successfully replicated. This method was used for checking the SDS solubility (or quantifying SDS concentration in feed solutions), but it was not suitable for quantifying the SDS in the collected permeate samples, since the measured conductivity in the permeate may be prevailed by the unrestrained sodium ions despite of the possible (partial) retention / adsorption of dodecyl sulfate chains in the membrane matrix.

Another method was to implement Stains-all dye (cf. section 3.4.2 and 4.3.1.6.3 c in the final W-UFO report). To determine the SDS concentration in the UF permeates, two calibration curves were established between  $UV_{453}$  and SDS concentration. This was done for SDS solutions that were prepared in two different background water matrices, ultrapure water as well as UF permeate (from filtration of surfactant-free emulsified oil at concentration of 10 mg/L). The calibration curves are presented in Figure 8a and b, respectively. Both calibration curves were obtained for SDS concentrations in the range of 0 - 100 mg/L with a step of 10 mg/L.

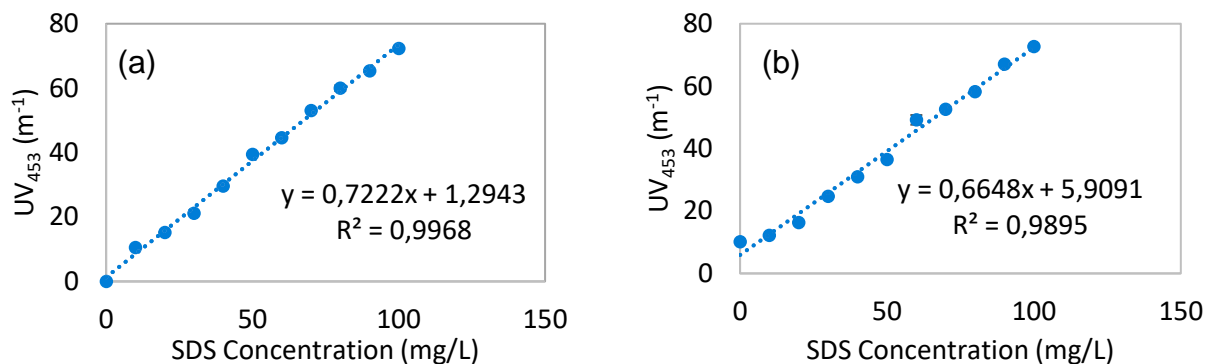


**Figure 8: Calibration curve of measured  $UV_{453}$  ( $m^{-1}$ ) against the SDS concentration (mg/L) for solutions prepared with two different background water matrices, (A) ultrapure water and (B) permeate of 10 mg/L surfactant-free emulsified oil permeate through SM membrane**

To investigate whether SDS is being retained by UF membranes or not, two filtration experiments were conducted. In which two feeds were implemented, oil-free SDS solution at concentration of 48 mg/L, and surfactant-modified emulsified oil at oil concentration of 10 mg/L and SDS concentration of 48 mg/L. Both feeds were filtered through SM membrane module at a constant flux of  $100 L/(m^2 \cdot h)$ . Permeate samples were collected after 1, 2, 3, 4, 5, 15, 30, and 45 min filtration intervals and analyzed for the SDS concentration. Results of SDS concentration in the permeates of both experiments are plotted in Figure 9a and b, respectively.

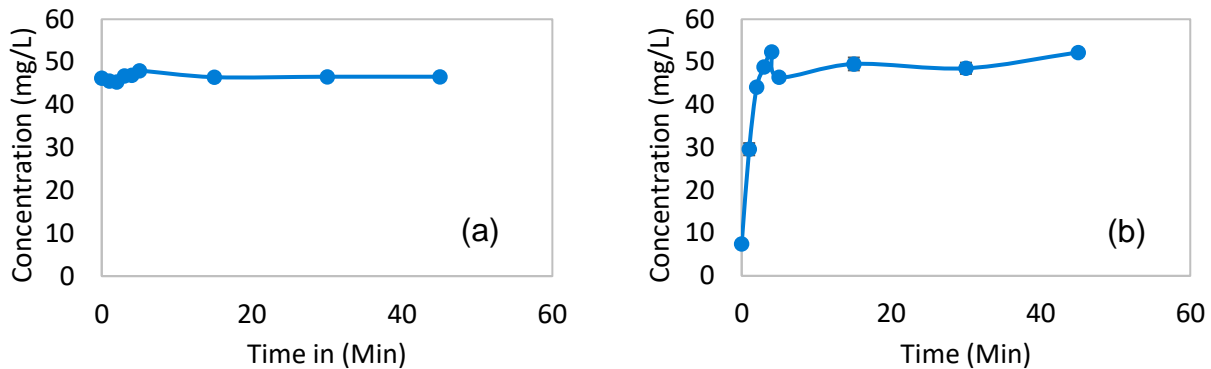


**Figure 9: Quantified SDS (mg/L) in the UF permeate against the filtration time (min) for (A) feed of 48 mg/L SDS without oil and (B) with emulsified oily feed at 10 mg/L as TOC through SM membranes**

Results from filtration experiments using oil-free SDS solution showed that the SDS concentration in permeate was almost equal to the feed concentration, indicating that no retention for SDS was achieved when oil-free SDS solution was filtered. On the other hand, different behavior was observed for surfactant-modified emulsified oil filtration. In the beginning of filtration experiments, partial retention of SDS was observed, then after almost 3 min of filtration, SDS concentration in the permeate was raised again to be close to its concentration in the feed. Such reduction (or partial SDS retention) should be attributed to SDS adsorption onto the retained emulsified oil droplets, which had positive effects on decreasing oil adhesion to the UF membrane and promotes fouling layer reversibility.

### 2.3.2.3 Influence of the quality of the applied SDS

In several experiments (over the course of the W-UFO project), three types of SDS products were implemented, those are  $\text{SDS}_{\text{VWR},21}$ ,  $\text{SDS}_{\text{VWR},23}$  and  $\text{SDS}_{\text{TS}}$ , cf. section 2.2.1. Notable differences were observed in the fouling behavior of PES membranes during the filtration of SDS-modified emulsified oils and oil-free SDS solutions. Consequently, the impacts of SDS quality on the membrane performance was investigated.

Three analytical techniques were applied to examine the quality of  $\text{SDS}_{\text{VWR},23}$  and  $\text{SDS}_{\text{TS}}$ : elemental analysis, FTIR spectroscopy, and CMC measurement, cf. section . Unfortunately, at the time of conducting these analysis there were no samples of  $\text{SDS}_{\text{VWR},21}$  remaining to be analyzed.

To investigate the reasons behind the observed differences, an elemental analysis was conducted to determine the carbon, hydrogen, nitrogen, and sulfur content in both SDS<sub>TS</sub> and SDS<sub>VWR,23</sub>. The measurements and the calculated theoretical values for pure SDS are presented in Figure 10.

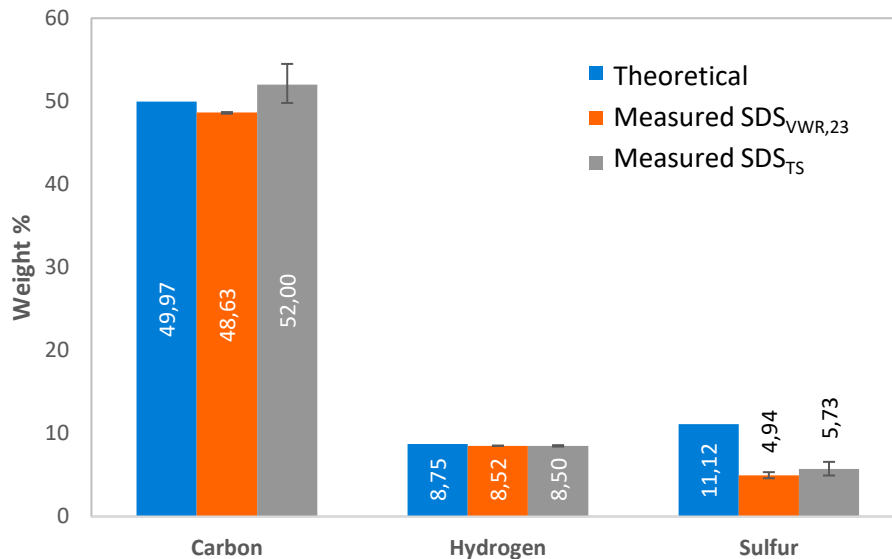


**Figure 10: Measured and calculated theoretical values for a pure SDS, and measured values for SDS<sub>VWR,23</sub> and SDS<sub>TS</sub> (Microanalytical Laboratory at University of Duisburg-Essen )**

It can be observed that the measurements for SDS<sub>VWR,23</sub> were slightly more reproducible compared to SDS<sub>TS</sub>, which exhibited higher fluctuations, bigger error values. However, it was also observed that neither SDS matched the theoretical values for pure SDS.

To further investigate the effect of impurities in SDS products, the CMC value for both SDS<sub>VWR,23</sub> and SDS<sub>TS</sub> was experimentally measured, alongside two reference SDS samples with purities of 95% and >99%, (cf. sections 3.4.3.3 and 4.3.1.7.1 c in final W-UFO report). SDS<sub>VWR,23</sub> exhibited a CMC value of 2.33 g/L, which is close to the expected typical CMC value for pure SDS. In contrast, the measured CMC value of SDS<sub>TS</sub> was 1.88 g/L, significantly deviating from the typical value and indicating the presence of impurities. Additionally, the surface tension of SDS<sub>TS</sub> at the final concentration was noticeably higher than normal, which indicates the presence of surfactant impurities. Further, it was observed that at lower concentrations, the surface tension of SDS<sub>TS</sub> decreased less

sharply. This behavior can be attributed to the presence of fatty alcohols, which generally have a relatively low CMC and contribute to the unusual characteristics of SDS<sub>TS</sub>. However, no significant differences in peaks intensities were noticed in FT-IR measurements. Inconsistent membrane performance was observed during the filtration of different types of SDS, i.e. SDS<sub>VWR,21</sub> SDS<sub>VWR,23</sub> and SDS<sub>TS</sub>. For instance, Figure 11a and b present two sets of filtration experiments of oil-free SDS solutions made of SDS<sub>VWR,21</sub> and SDS<sub>VWR,23</sub>. It was noticed that Different membranes performance can be clearly seen.

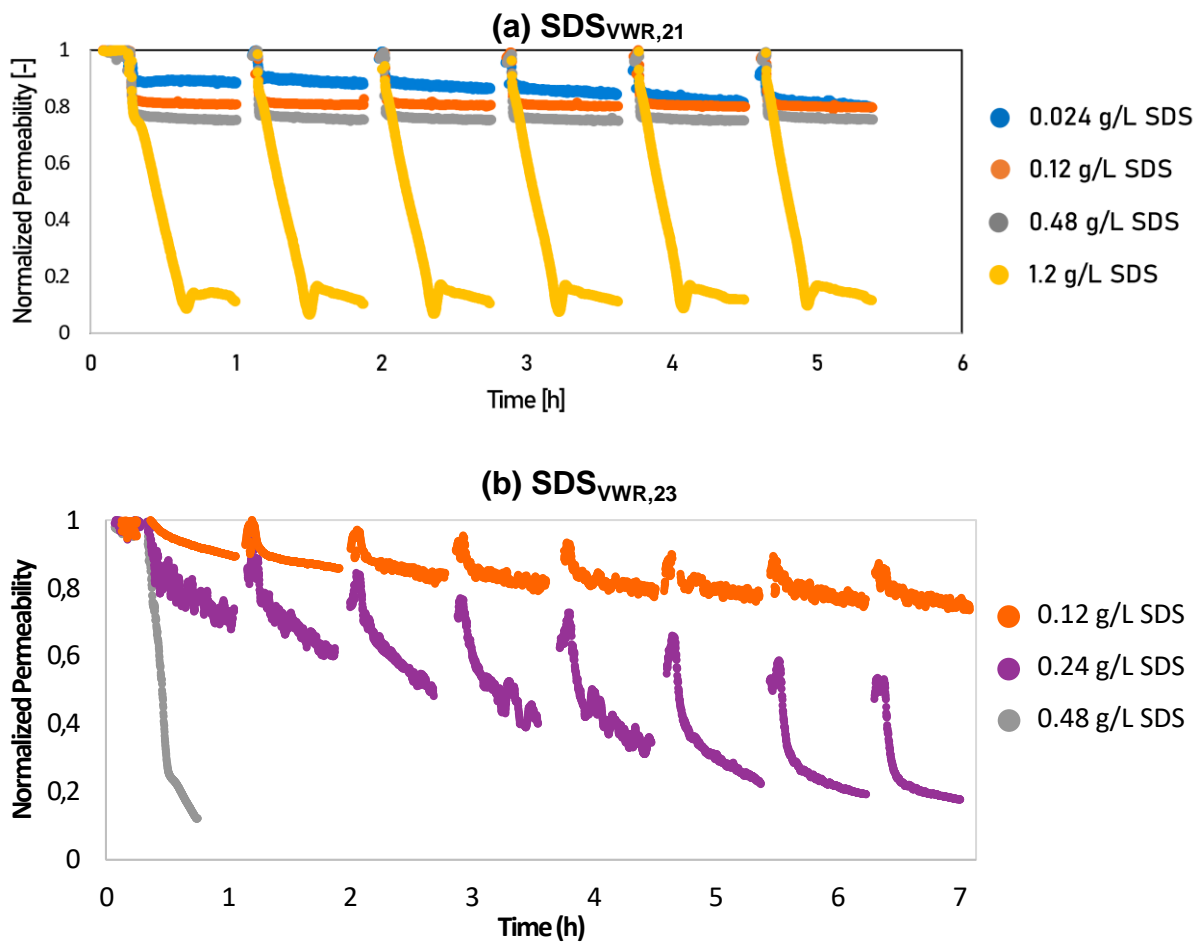


**Figure 11: Normalized permeability curves for SM membranes in filtration tests with multiple-cycles at a constant flux of 100 L/(m<sup>2</sup>·h) using oil-free SDS solutions of different concentrations (0.024 - 1.2 g/L) made of (A) SDS<sub>VWR,21</sub> and (B) SDS<sub>VWR,23</sub>,**

In the first set of experiments (Figure 11a), the membrane permeability was completely restored after each backwash for all tested concentrations. But this was not noticed in the second set (Figure 11b), a certain irreversible fouling remained after each backwash for

all three tested concentrations. On the other hand, different fouling rates were observed within the filtration cycles. Similarly, two sets of filtration experiments with surfactant-modified emulsified oils and oil concentration of 10 and 25 mg/L and 0.48 g/L were conducted with  $\text{SDS}_{\text{VWR},21}$  and  $\text{SDS}_{\text{VWR},23}$  ,. As indicated in Figure 12, higher fouling rate within the cycle could be noticed when using the  $\text{SDS}_{\text{VWR},23}$  compared to  $\text{SDS}_{\text{VWR},21}$ . Also, higher permeability recovery was noted after each backwash with  $\text{SDS}_{\text{VWR},21}$ .

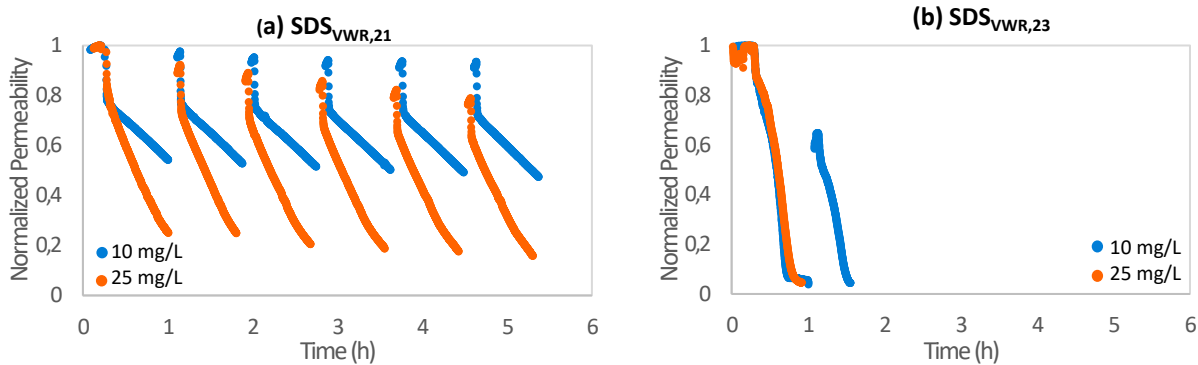


**Figure 12: Normalized permeability curve for filtering surfactant-modified emulsified oil with 10 mg/L and 25 mg/L both with 0.48 g/L of (A)  $\text{SDS}_{\text{VWR},21}$  and (B)  $\text{SDS}_{\text{VWR},23}$ . One trial each**

On the other hand, two experiments were conducted using SM membranes as well, in which  $\text{SDS}_{\text{TS}}$  at concentration of 0.24 g/L was implemented. One experiment was conducted using oil-free SDS solutions and the other one using SDS-modified emulsified oil at oil concentration of 10 mg/L. As indicated in Figure 13, both experiments suffered from very severe permeability decline, so that the membrane lost over 95% of its permeability within the first cycle. Thereafter both experiments were aborted as when the pressure exceeded the maximum allowed pressure of 4 bar.

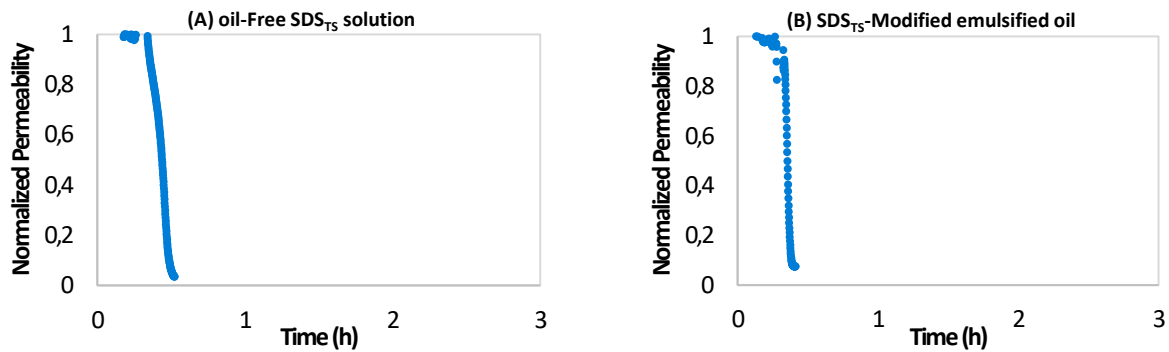


**Figure 13: Normalized permeability curve for filtering (A) oil-free SDS<sub>TS</sub> solutions and (B) SDS<sub>TS</sub>-Modified emulsified oil with oil concentration of 10 mg/L, both at SDS concentration of 0.24 g/L through SM membranes, one trial each**

This different behavior of SDS<sub>TS</sub>, compared to SDS<sub>VWR,23</sub> can be attributed to the presence of impurities, likely fatty alcohols, as indicated by the elemental and CMC analyses. This finding further emphasizes that the SDS-enhanced dead-end ultrafiltration method is highly sensitive and strongly intolerant to deviations in the experimental setup, such as variations in SDS quality.

One possible reason for the inconsistent behavior of filtering SDS<sub>VWR,21</sub> and SDS<sub>VWR,23</sub> could be potential differences in the membrane batches implemented in 2021 and 2023. For that further investigations were carried out on the SDS-enhanced dead-end ultrafiltration method. In which another PES UF membrane type from different manufacturer were tested, namely X-Flow membranes, cf. section 2.2.2.

Figure 14a and b illustrate the normalized permeability curves for mini-plant filtration experiments using oil-free SDS solutions and surfactant-modified emulsified oil with oil concentration of 10 mg/L, both made with SDS<sub>VWR,23</sub> at concentration of 0.24 g/L through SX membranes, respectively.



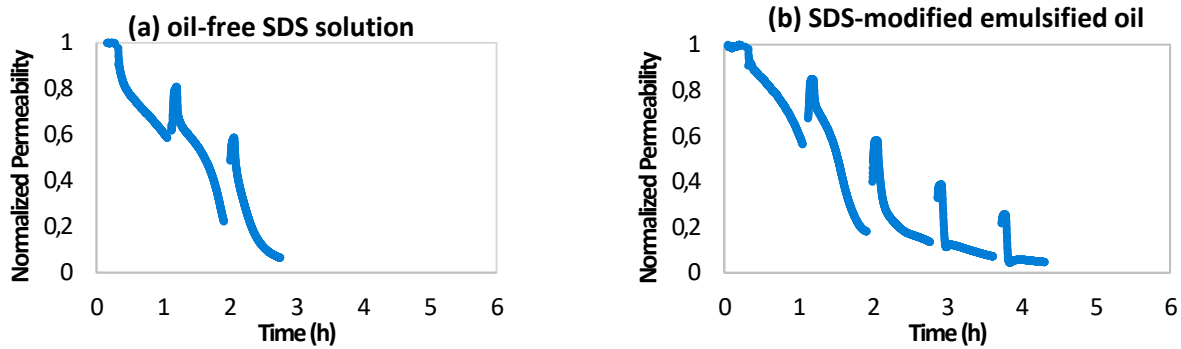


**Figure 14: Normalized permeability curve for filtering (a) oil-free SDS solutions and (b) SDS-modified emulsified oil with oil concentration of 10 mg/L, both made with SDS<sub>VWR,23</sub> at concentration of 0.24 g/L through SX membranes, one trial each**

Despite the differences in permeability decline rates within the cycle and the recovery rate after backwash, the overall filtration trends observed with SX membranes were comparable to those with SM membranes. These differences can be attributed to variations in the manufacturing processes, such as blending techniques or membrane post-treatment, as well as deviations in SDS quality.

However, it was not possible to conduct experiments implementing SDS<sub>VWR,21</sub> and SX membranes because no SDS<sub>VWR,21</sub> samples were remaining or possible to procure. So that the not favorable filtration behavior of SDS solutions and SDS-modified emulsified oils reported in the section are very likely related to the deficits in the SDS quality but not of the SX or SM membranes.

#### ***2.3.2.4 Influence of filtration conditions on the efficiency of surfactant-enhanced dead-end ultrafiltration***

Based on the findings reported in W-UFO II regarding the surfactant-enhanced dead-end ultrafiltration method, further investigations were planned to examine the influence of filtration conditions on the efficiency of the developed method. This included a total of 70 experiments conducted under varying operational conditions, specifically: filtration flux, filtration duration, BW flux, BW duration, and the duration of the pure water filtration step following the BW. These experiments aimed to optimize the listed parameters by evaluating their impact on the efficiency of the surfactant-enhanced dead-end ultrafiltration process. This was planned to be carried out with the help of a statistical experimental plan to test filtration fluxes in the range of 60 – 140 L/(m<sup>2</sup>·h), filtration cycle durations in the range

of 30 -60 min, backwashing fluxes in the range of 160 - 300 L/(m<sup>2</sup>·h), backwashing duration in the range of 30 - 90 s, and post pure water. filtration durations in the range of 0 - 10 min (with a flux equal to the filtration flux). This results in 46 experiments. Thereafter, about 10 – 15 further experiments were planned to validate the output of the experimental design. In addition to about 10 experiments for optimizing the dosing conditions. So that, a total of about 70 experiments was dedicated to this part, i.e. these two subtasks, in the proposed plan, see WP2, subtasks b and c, page 22 in W-UFO III+ proposal.

During the execution of the project, over 100 experiments were carried out in relation to this subtask. This was realized using three filtration units: Poseidon, Neptunus and Playground, and using three types of membrane modules: SM, SM<sub>2</sub> and SX. However, as previously mentioned in section 2.3.2.3, the surfactant-enhanced dead-end ultrafiltration method was sensitive to alternations in the experimental set up, mainly the quality of the SDS applied. This unforeseen significant fluctuations in the materials and the related variations in performance parameters necessitated an adjustment and expansion of the experimental plan. We decided to suspend the development of mathematical relationships through statistical experimental design and instead conduct more individual experiments with direct parameter comparisons to reliably capture trends. This caused additional workload and material costs. For example, Table 3 shows a list of 17 experiments that were carried out using Playground filtration unit out of the 46 planned experiments according to the design of experiment (see section 3.10.3 in the final W-UFO report). The total fouling at the end of the experiment was utilized as the output parameter for these experiments. All experiments in this section, i.e., section 2.3.2.4, were conducted utilizing SDS<sub>VWR,23</sub>.

**Table 3: A list of experiments completed in accordance with the statistical experimental plan with central composite design and the associated filtration flux, filtration cycle duration, backwash flux, backwash duration, and pure water filtration including experiments done on playground, number of successful cycle and total fouling.**

Experiment number	Filtration flux (L/m <sup>2</sup> ·h)	Filtration cycle duration (min)	Backwash flux (L/m <sup>2</sup> ·h)	Backwash duration (sec)	pure water filtration (min)	Nr. of successful cycle	Total fouling
EXP 01	60	30	90	30	3	6	79%
EXP 02	140	30	90	30	3	3	75%

<b>EXP 03</b>	60	60	90	30	3	3	81%
<b>EXP 05</b>	60	30	230	30	3	6	41%
<b>EXP 06</b>	140	30	230	30	3	1	85%
<b>EXP 07</b>	60	60	230	30	3	3	57%
<b>EXP 08</b>	140	60	230	30	3	1	86%
<b>EXP 09</b>	60	30	90	90	3	6	42%
<b>EXP 10</b>	140	30	90	90	3	6	69%
<b>EXP 11</b>	60	60	90	90	3	3	82%
<b>EXP 13</b>	60	30	230	90	3	6	71%
<b>EXP 14</b>	140	30	230	90	3	6	65%
<b>EXP 15</b>	60	60	230	90	3	3	44%
<b>EXP 16</b>	140	60	230	90	3	1	80%
<b>EXP 17</b>	60	30	90	30	7	6	47%
<b>EXP 19</b>	60	60	90	30	7	3	58%
<b>EXP 23</b>	60	60	230	30	7	3	
<b>EXP 43</b>	100	45	160	60	5	4	58%
<b>EXP 46</b>	100	45	160	60	5	4	76%

In conclusion, it was noted that tests conducted under the applied conditions in this section demonstrated no enhancement in performance when altering the filtration fluxes, filtration cycle durations, backwashing fluxes, backwashing duration and post pure water after backwash. This lack of improvement is likely attributable to the previously discussed issues with the surfactant-enhanced dead-end UF process, as resulting from variations in SDS quality, as detailed in previous section 2.3.2.3.

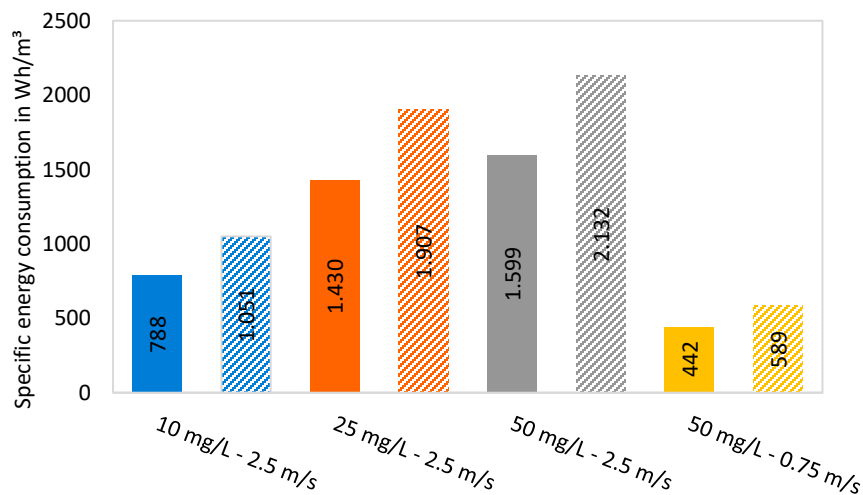
### **2.3.2.5 Economic and environmental assessment**

To estimate the difference in the energy consumption, between the crossflow operation and the surfactant-enhanced UF dead-end operation methods, the specific energy consumption per each cubic meter of produced permeate was calculated for each process as it was indicated in section 3.11 in the final W-UFO report.

Four filtration experiments in which surfactant-free emulsified oils were filtered at concentrations of 10, 25 and 50 mg TOC/L with SM membranes at crossflow velocity (CFV) of 2.5 m/s or 0.75 m/s were analyzed again to evaluate the specific energy consumption for crossflow operation. The economic assessment of the surfactant-enhanced dead-end UF

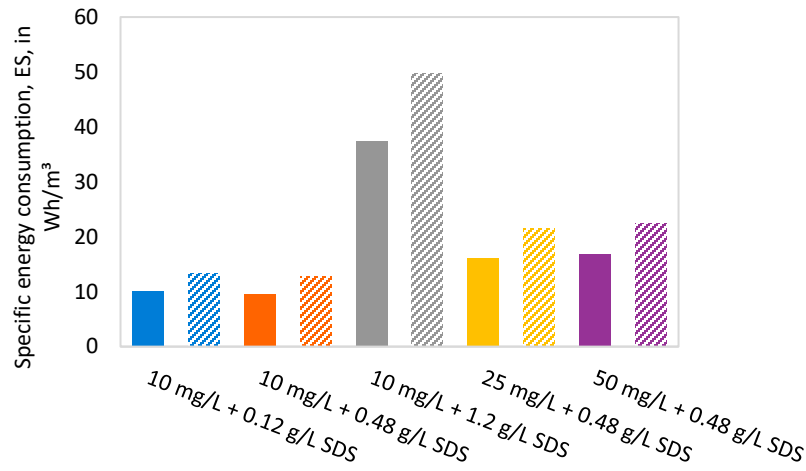
was conducted based on the experiments demonstrating the best reproducible performance. For that the results from five experiments were selected and analyzed for economic sustainability calculation. These five experiments comprised three trials with an oil concentration of 10 mg/L and SDS concentrations of 0.12, 0.48, and 1.2 g/L. Along with two other trials that were conducted implementing oil concentrations of 25 and 50 mg/L, both conducted with an SDS concentration of 0.48 g/L. The filtration behavior of both sets of experiments for crossflow and dead-end were discussed in detail in sections 4.4.1.1 and 4.4.1.2 in the final W-UFO report, respectively.

Figure 15 presents the calculated EN<sub>s</sub> values for the four crossflow experiments assuming an  $\eta_F$  of 0.6 or 0.8 and that an energy recovery is implemented on the concentration side. It was observed that higher specific energy consumption was associated with higher oil concentrations. Assuming a pump efficiency factor of  $\eta_F$  of 0.8, approximately 788, 1,430 and 1,599 Wh/m<sup>3</sup> were needed for feed containing oil at concentrations of 10, 25, and 50 mg/L, respectively. Although no significant difference in fouling behavior was observed when the CFV was reduced to 0.75 m/s, but a substantial decrease in energy consumption was evident, amounting to 442 Wh/m<sup>3</sup>. The lower efficiency factor  $\eta_F = 0.6$  resulted in increased energy consumption.



**Figure 15:** Specific energy consumption of crossflow experiments with emulsified oils at concentration of 10, 25 and 50 mg<sub>TOC</sub>/L at CFV of 2.5 m/s. Calculated for  $\eta_F = 0.8$  (solid-colored) and 0.6 (hatched)

Figure 19 illustrates the specific energy consumption of the surfactant-enhanced dead-end ultrafiltration experiments also calculated for two pump efficiency values of 0.8 and 0.6. For experiments with an oil concentration of 10 mg/L and SDS dosages of 0.12, 0.48, and 1.2 g/L,  $E_s$  were 10, 9.6, and 37 Wh/m<sup>3</sup>, respectively, for a pump efficiency of 0.8.



**Figure 16: Specific energy consumption of surfactant-enhanced dead-end UF experiments with surfactant-enhanced emulsified oils at a concentration of 10 mg/L with SDS concentration of 0.12, 0.48 and 1.2 g/L and an oil concentration of 25 and 50 mg/L with SDS concentration of 0.48 g/L. Calculated for  $\eta_F = 0.8$  (solid-colored) and 0.6 (hatched)**

Two representative experiments, one for each operation mode, were selected for further  $EN_s$  calculation. The first experiment, labeled EXP<sub>CFW</sub>, was conducted using crossflow mode with an oil concentration of 10 mg/L and CFV of 2.5 m/s. The second experiment, labeled EXP<sub>DE</sub>, was conducted using dead-end mode with the same oil concentration but an SDS dosage of 0.48 g/L. Fehler! Verweisquelle konnte nicht gefunden werden. Fehler! Verweisquelle konnte nicht gefunden werden. provides more detailed operation conditions of each one of these experiments.  $\Delta EN$  and  $\Delta C_{SDS}$  for these both experiments were calculated as follows:

$$\Delta EN_S = EN_{S,CFW} - EN_{S,DE} = 788 \text{ Wh/m}^3 - 9.6 \text{ Wh/m}^3 \approx 778 \text{ Wh/m}^3$$

$$\Delta C_{SDS} = C_{CFW} - C_{DE} = 0 - C_{DE} = -C_{DE} = -0.48 \text{ g/L}$$

These values were used in the further assessment.

The cost of SDS depends on various factors, such as the source of SDS (petrochemicals, oleochemicals, etc.), its production lifecycle, and the production site or location. The price

for 1 kg of SDS from three marketplaces for suppliers of industrial level, namely: Alibaba, Made-in-china and Global Sources was found about 0.65, 0.83 – 1.3 and 0.83 – 1.57 €/kg, which corresponds to a minimum ordered quantity of 20, 20 and 5 ton, respectively.

Considering an average price of 1.1 € per kg, the cost difference due to the SDS dosage can be calculated as follows:

$$\Delta Cost_{SDS} = \Delta C_{SDS} \cdot Cost_{SDS} = -0,48 \text{ g/L} \cdot 1.1 \text{ €/kg} = -0.264 \text{ €/m}^3$$

The cost balance between the crossflow and surfactant enhanced dead-end UF operation was calculated as described in section 3.11 in the final W-UFO report. The two main factors still needed to be defined are the unit price of energy and the unit price of SDS. The electricity price depends on the location and the source of energy. Table 4 lists the electricity price, the respective value for  $\Delta Cost_{EN}$  considering an energy consumption of 0.758 kWh/m<sup>3</sup> and the  $\Delta Cost$  considering an average SDS cost of 0.264 €/m<sup>3</sup> for Germany, Saudi Arabia, Egypt and Sweden.

**Table 4: Electricity price, the respective value for  $\Delta Cost_{EN}$  considering an energy consumption of 0.778 kWh/m<sup>3</sup> and the  $\Delta Cost$  considering an average SDS cost of 0,264 €/m<sup>3</sup> for Germany, Saudi Arabia, Egypt and Sweden.**

Country	Electricity price in €/kWh	$\Delta Cost_{EN}$ in €/m <sup>3</sup>	$\Delta Cost$ in €/m <sup>3</sup>
Germany	0.1178	0.092	-0.172
Saudi Arabia	0.069	0.054	-0,210
Egypt	0.037	0.029	-0,235
Sweden	0.07	0.055	-0,209

It can be observed that  $\Delta Cost$  is negative, where  $|\Delta Cost_{EN}| < |\Delta Cost_{SDS}|$ . This indicates that the costs associated with the SDS dosage in the dead-end operation are higher than the cost compared to the crossflow operation. In conclusion, the SDS dosage cost is more than three times higher than the energy cost difference, resulting in the fact that even reducing the SDS dosage, e.g., to 0.24 g/L, the surfactant-enhanced dead-end ultrafiltration process will still be economically unfeasible.

Based on the literature review about the CFP value of the produced energy, cf. section 3.11, for further calculations, the average CFP value for EU in 2022 was considered and used, i.e.,  $CFP_{EN} = 0.251 \text{ kg CO}_2\text{eq/kWh}$ .

Calculating the CFP for SDS was found to be more challenging than for electrical energy. Despite the widespread use of SDS, there is a notable lack of quantitative data regarding its environmental impacts. However, an estimation value was defined and compared based on a literature review (cf. section 4.4.2.1 in the final W-UFO report). Referring to the case study of surfactant chain production of Sodium Lauryl Ether Sulfate containing 3 mol of ethylene oxide (SLES 3EO) reported by Nogueira et al. (2019) [36]. As a result, the  $CFP_{SDS}$  was estimated about 1,590 kg CO<sub>2e</sub>/t. Thus, the total CFP difference is:

$$\begin{aligned}\Delta CFP &= \Delta CFP_{EN} + \Delta CFP_{SDS} = 0,195 \text{ kg CO}_2\text{e/m}^3 - 0.763 \text{ kg CO}_2\text{e/m}^3 \\ &= -0.568 \text{ kg CO}_2\text{e/m}^3\end{aligned}$$

A similar observation as for the  $\Delta$ Cost can also be made for the  $\Delta$ CFP, namely that the difference indicates a negative value. This implies that the CFP associated with surfactant-enhanced dead-end UF operation exceeds that of the crossflow operation. Furthermore, the use of SDS results in the release of over four times the amount of carbon compared to the additional energy required in crossflow. Hence, it is apparent that the surfactant-enhanced dead-end approach has a more significant environmental impact.

### 2.3.3 Hybrid UF processes with PAC dosing and/or coagulants

#### 2.3.3.1 Adsorption kinetic experiments

To investigate the adsorption behavior, a series of adsorption kinetic experiments were performed with three commercially available granular activated carbon products, ABG-H, HMA-B and ORG-K, made from the different raw materials wood, anthracite, and coconut shells, respectively. First, the granular activated carbon products were milled into PAC with a comparable particle size ( $D_{50,v} = 5 \sim 8 \mu\text{m}$ ). As shown in Figure 17, at 50 mg/L dosage rate of PAC, the PACs removed 75%, 58%, and 53% of the  $UV_{254}$  of the oil emulsion at concentration of 25 mg/L an input concentration of  $65 - 70 \text{ m}^{-1}$  as  $UV_{254}$ .

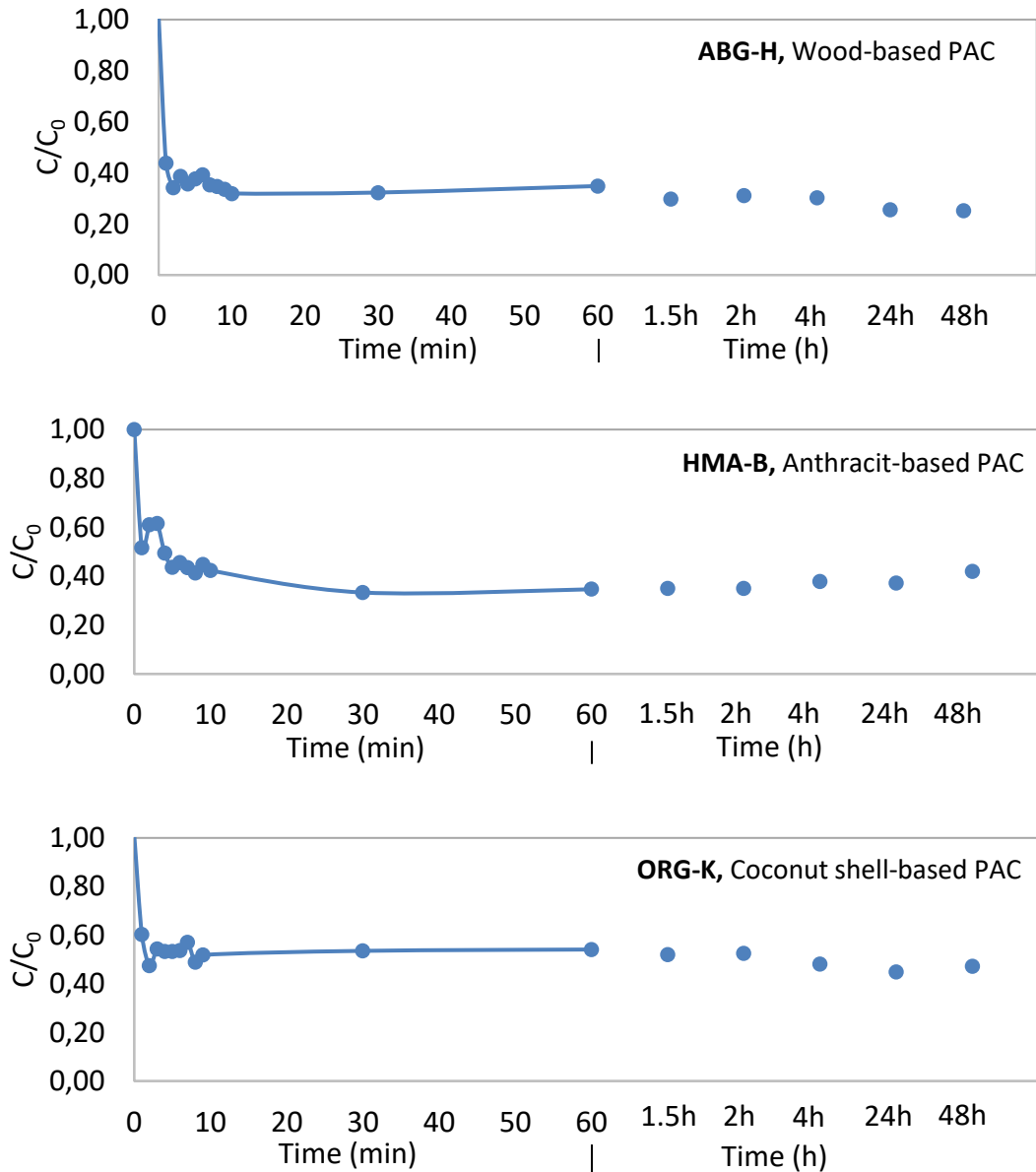


**Figure 17: Results of adsorption kinetic experiments of ABG-H, HMA-B and ORG-K PACs, presented as  $UV_{254}$  concentration in the permeate (C) related to the feed concentration ( $C_0$ ) over time**

The differences in the removal of  $UV_{254}$  using the three PACs are comparable to the removal of  $UV_{254}$  when the same PACs are applied to municipal wastewater (68%, 55%, and 37% at an input concentration of  $27 \text{ m}^{-1}$ ). The three PACs differ mainly in their surface area formed by meso- and macropores (822, 424 and  $279 \text{ m}^2/\text{g}$ ). The micropore surface area of the three PACs, on the other hand, is comparatively similar at 787, 741, and  $888 \text{ m}^2/\text{g}$ , respectively, or exhibits a different sequence. The removal of oil compounds identified as  $UV_{254}$  is therefore can be expected, based on these results, to occur either



on the outer surface or in the meso- and macropores of PAC. However, due to the irreproducible adsorption behavior on the PAC during the adsorption isotherms experiment (see following paragraph and section 4.3.2.2 in the final W-UFO report) it is more likely that the adsorption to occur on the outer surface of the PAC, rather than inside the pores. A set of experiments were carried out to obtain the adsorption isotherm and to define the minimum required dose of PAC to achieve the highest possible oil removal. PAC concentration varied first in the range of 1-100 mg/L with a step of 10 mg/L. The removal of oil in terms of  $UV_{254}$  are depicted in Figure 18. The results of these experiments showed that all PAC behaves similar with a strong increase of the elimination at low dosage up to 10 mg/L and then decreasing elimination rate with increasing dosage. Up to a dosage of 50 mg/L, the elimination of ORG-K is about 10 % better than that of the other PAC types. Above a PAC dosage of 50 mg/L, elimination remains constant at around 80% for all PAC types.

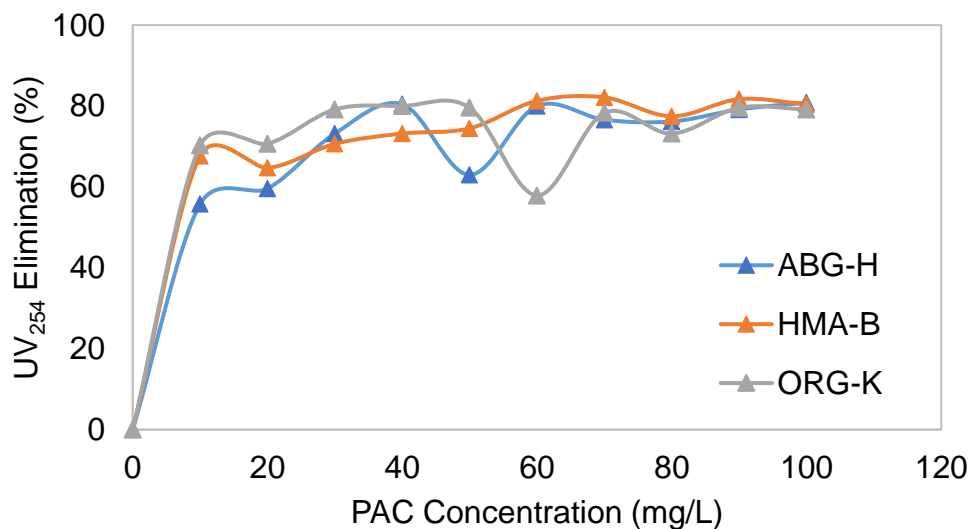


**Figure 18:**  $UV_{254}$  elimination in percentage against the direct dosed concentrations of three PACs, ABG-H, HMA-B and ORG-K to the emulsified oil of 25 mg/L as TOC, one trial each

It seems that the oil sample has about 20% components that are not adsorbable, so it is a multi-component system. Furthermore, the PAC types differ slightly in their maximum loading at PAC dosing quantities below 10 mg/L. Contrary to the results from the kinetics tests, ORG-K has the best elimination in this dosing range with ca. 70%. However, repeating these experiments resulted in very high fluctuations (see section 4.3.2.2 in the

final W-UFO report). In general, no clear trend can be drawn out of these isotherms. This can be attributed to the fact that crude oil contains several components, and the final isotherm is expected to be a multi-component isotherm. But it can be assumed that the main adsorption takes place on the outer surface of the activated carbon and only a negligible capacity of the large inner surface of the PAC is used. It is assumed that the oil droplets are adsorbed on the outer surface and coalesce with the next droplets faster than they can diffuse into the interior of the PAC. As a result, the large oil droplets also block the access of smaller oil components to the inner structure of the PAC.

### ***2.3.3.2 Coagulation/Flocculation experiments***

To determine the optimum coagulation/flocculation parameters for better membrane performance and oil removal, a series of typical jar-test coagulation experiments (according to W 218 DVGW [46]) were carried out with different commercial iron- and aluminum-based inorganic coagulants (0 - 12 mg/L for iron and 0 - 6 mg/L for aluminum). As presented in Figure 19, the aluminum-based coagulant showed little to no removal for the oil at all coagulant dosing concentrations, whereas the iron-based coagulant was able to remove about 20% of the DOC even at a dosing concentration of about 1 mg/L. However, increasing the dosing concentration did not result in a further significant change in oil removal. Similar to the adsorption tests, there appears to be an oil fraction that cannot be flocculated.

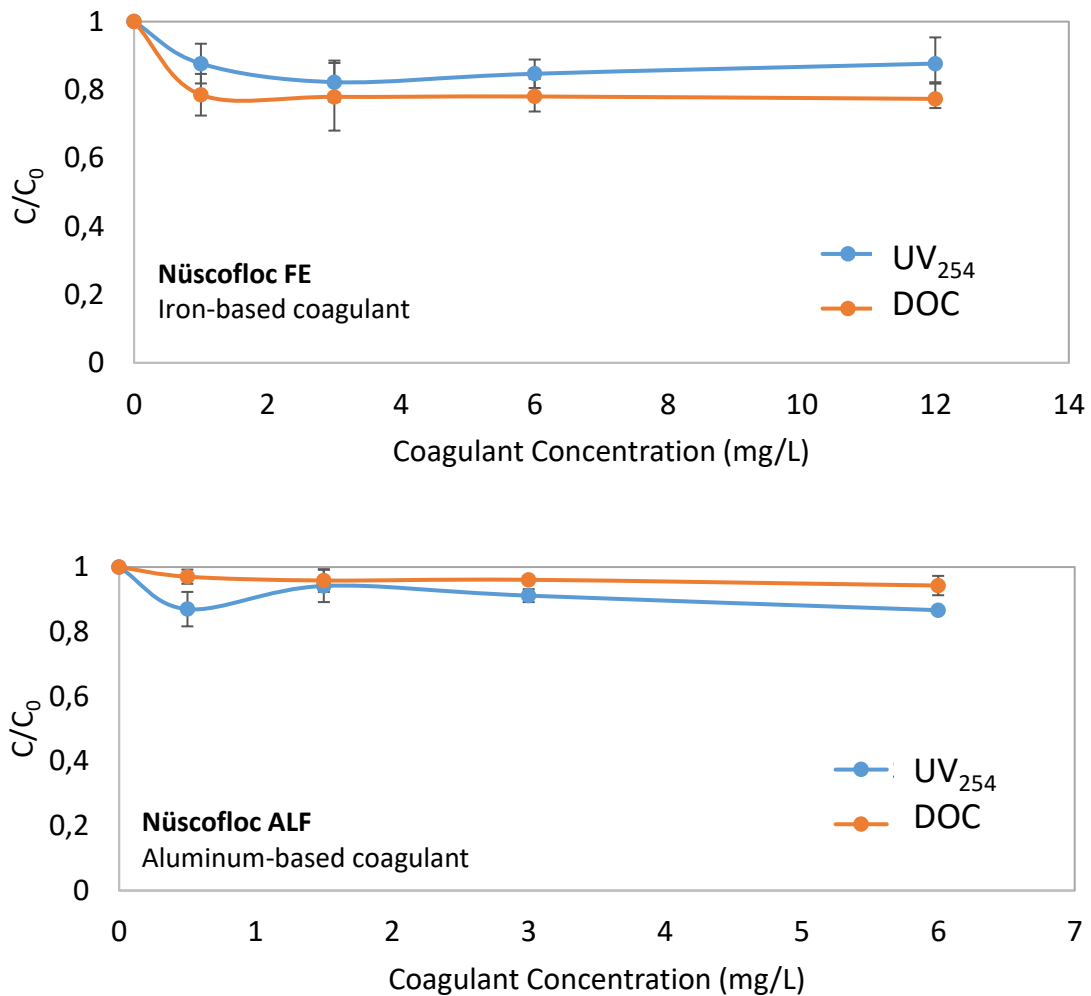


**Figure 19:** Relative concentrations of oil as DOC and UV<sub>254</sub> in the supernatant of the coagulation/flocculation experiments (C) related to the feed concentration (C<sub>0</sub>) for Nüscofloc FE as iron-based coagulant and (b) Nüscofloc ALF as aluminum-based coagulant. Presented as average of two trials with the min. and max. error bars.

For the further studies on the combination of UF with coagulants, the iron-based coagulant was chosen as it showed better oil removal than the aluminum-based one. The dosage of the iron-based coagulant was set to 1 – 2 mg/L, as this concentration was sufficient to achieve an additional oil removal of about 20% with respect to DOC and UV<sub>254</sub>.

### 2.3.3.3 Filtration tests using S100 flat sheet MF membranes

To investigate the efficiency of implementing hybrid process, different operation configurations were tested using on three membranes S100 (MF), UP150 (UF) and SM<sub>1</sub> (UF)

membranes. This was conducted as Standalone membrane, PAC-membrane, coagulation-membrane and coagulation-PAC-membrane.

Figure 20a, b, c and d show the normalized permeability curves against the specific filtered volume per membrane area ( $V$ ) in  $L/m^2$  for filtration experiments of standalone S100, combination of coagulation-S100, PAC-S100 and coagulation-PAC-S100, respectively. All filtration experiment were performed at constant pressure of 1 bar with surfactant-free emulsified oil with an oil concentration of 25 mg/L as TOC.

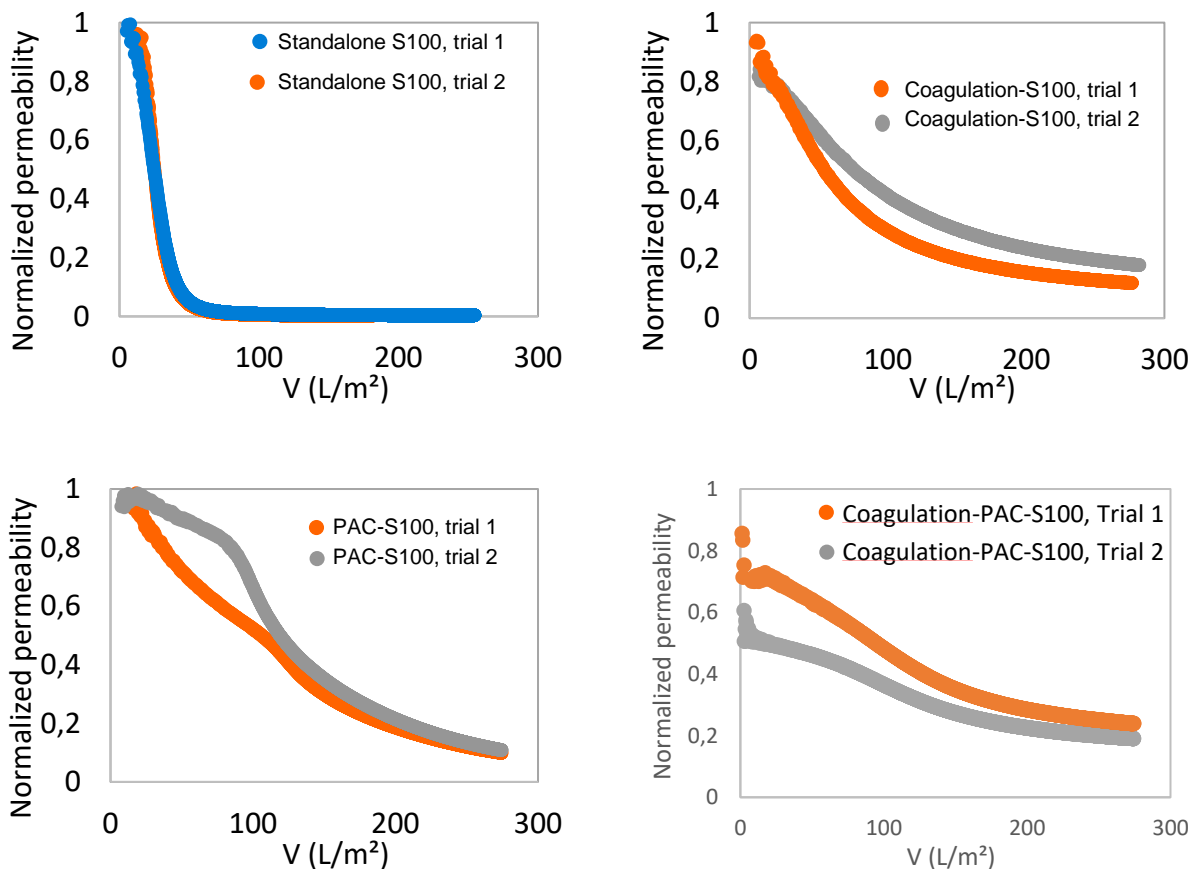


**Figure 20: Normalized permeability curve of the dead-end filtration experiments on standalone S100, combination of coagulation-S100, PAC-S100 and coagulation-PAC-S100 for emulsified oils of 25 mg/L as TOC at constant pressure of 1 bar**

The results show that the use of PAC and/or coagulation in the feed of an MF significantly reduces the fouling of the membranes compared to the application of MF alone. Under the conditions tested, PAC-MF resulted in less fouling than coagulation-MF. Although the

combined PAC-coagulation-MF showed slightly higher fouling at the beginning of the trial, it resulted in the lowest fouling rate at the end of the trial period.

Similar experiments using UP150 membranes were also conducted (see section 4.3.2.5 in final W-UFO report). The results demonstrated that the application of PAC and/or coagulation prior to a UF significantly reduced fouling compared to the use of UF alone. Unlike the tested MF, the coagulation-UF resulted in less fouling than the PAC-UF and the PAC-coagulation-UF exhibited the lowest fouling rate. The difference between MF and UF membranes can be attributed to the larger pore size of MF which may allow small-formed flocs to cause pore blockage. The best results with the combination of PAC and coagulation in both MF and UF could be due to the gradual development of a protective layer over the membrane, which in case of MF prevents small flocs from penetrating and blocking the pores.

After investigating the influence of PAC dosage and/or coagulation prior to flat sheet S100 and UP150 membranes, the next objective was to assess the improvement in backwash efficiency. To achieve this, a series of filtration experiments were conducted on capillary SM<sub>1</sub> membranes at a constant pressure of 0.4 bar. The experiments were conducted in four combinations: standalone SM membrane, PAC-SM, coagulation-SM, and PAC-coagulation-SM, with each cycle followed by a one-minute backwash step at a pressure of 1 bar. Figure 21 shows the results of experiments of standalone UF and coagulation-UF experiments.

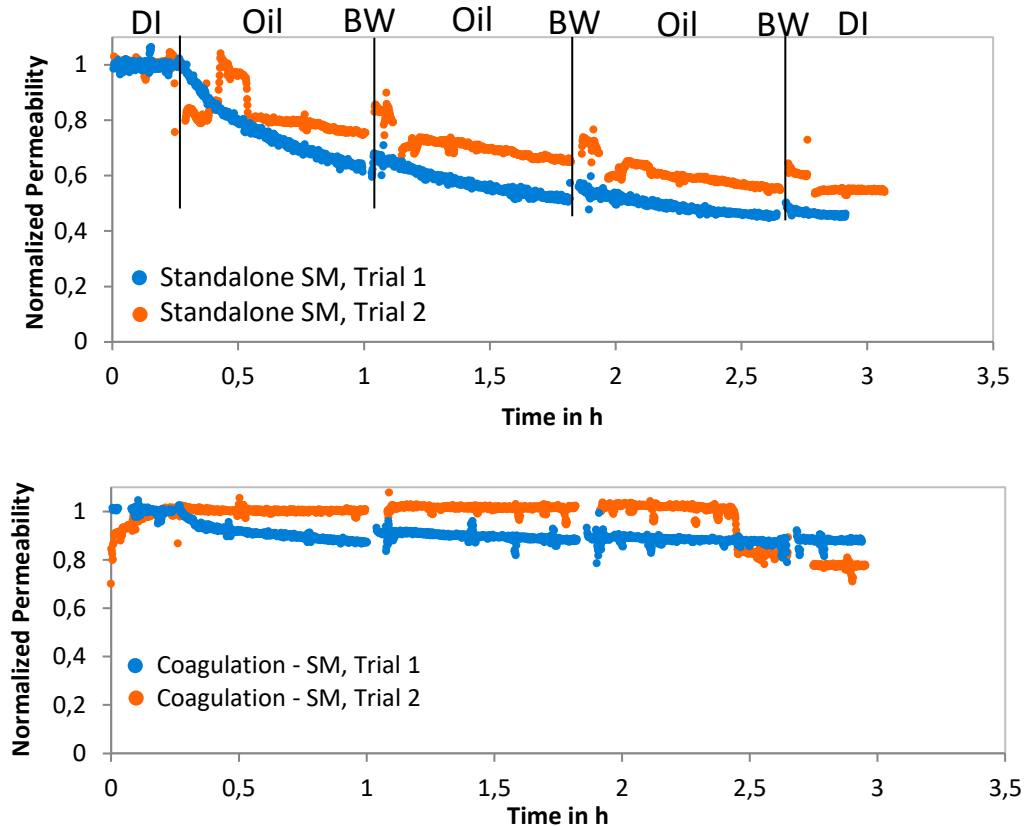


**Figure 21: Normalized permeability curve for filtering surfactant-free emulsified oil of 10 mg/L as TOC at constant pressure of 0.4 bar as standalone SM<sub>1</sub> or as combination of coagulation-SM<sub>1</sub> with Nüscofloc FE coagulant at dosage of 1 mg/L**

It was noticed that dosing coagulant prior to UF membranes reduced the fouling rate within the filtration cycle but no significant improvement in the backwash efficiency could be proved. However, long-term experiments were needed to prove such finding. Both PAC-UF and coagulation-PAC-UF that were conducted on SM<sub>1</sub> membranes, showed higher fouling rate than the coagulation-UF operation (cf. section 4.3.2.6 in final W-UFO report).

To investigate the influence of PAC and/or coagulant dosage on UV<sub>254</sub> elimination, one feed sample and two or three permeate samples were collected and analyzed for UV<sub>254</sub> absorbance. Figure 22 presents the UV<sub>254</sub> elimination results for standalone SM and hybrid operations of PAC-SM, coagulation-SM, and coagulation-PAC-SM systems.

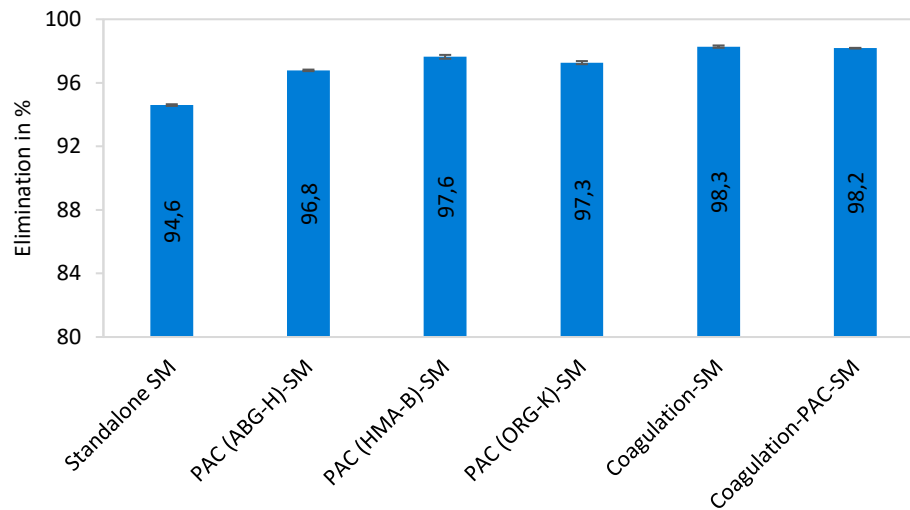


**Figure 22: Elimination performance represented as percentage retention of UV<sub>254</sub> for standalone S100, PAC-S100, coagulation-S100 and PAC-coagulation-S100**

The highest elimination efficiency could be noticed in case of coagulation-UF or coagulation-PAC-UF operation. The better elimination in coagulant dosing compared to PAC may be related to the improved size exclusion after coagulant dosing, as the coagulant helps to form larger oil droplets or clusters of small droplets. In addition, the ability of PAC to adsorb all oils is limited as adsorption occurs mainly on the outer surface of the PAC particles.

### 2.3.4 Experiments relevant to practice

To assess the scalability of the results obtained, selected experiments were carried out with membrane modules that have a similar length to the real modules, a larger surface area and a longer time span. Figure 23 shows the permeability of filtering surfactant-free emulsified oils at oil concentration of 10 mg/L through pristine LM<sub>2</sub> modules. This was conducted as standalone UF in dead-end at constant flux of 100 L/(m<sup>2</sup>·h). A sharp decline in the permeability was noticed, in which the membrane permeability dropped to about 267, 147 and 53 L/(m<sup>2</sup>·h·bar), respectively. The membrane lost about 88% of its permeability after less than 3 hours, which is higher than the fouling rate that was noticed in similar experiments that were carried out with SM modules, in which the membrane lost about

60% of its permeability after 3 hours (see Figure 47, cf. section 4.3.1.2.2). However, the experiment was not conducted continuously; the experiment paused at several time points, indicated as points A-E in Figure 23. The filtration was first paused after approximately 2.9 hours (Timepoint A) due to the pressure exceeding the maximum allowed limit of 2.5 bar. Significant fouling necessitated manual CIP of the membrane. This was accomplished by rinsing with a 1.2 g/L SDS solution for 15 minutes, followed by a 10-minute rinse with pure water. Data from this step were not recorded.

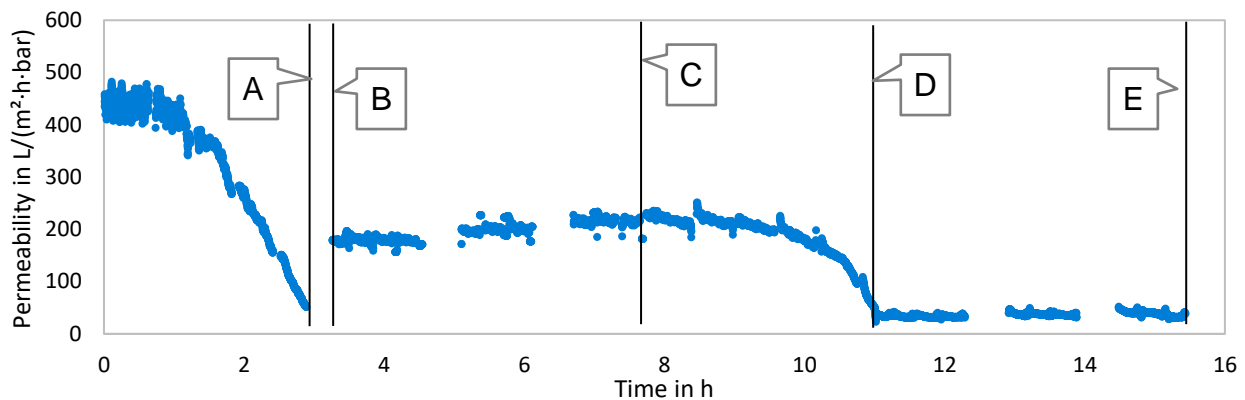


**Figure 23: Permeability of filtering surfactant-free emulsified oils at oil concentration of 10 mg/L through LM<sub>2</sub> membranes as standalone UF at constant flux of 100 L/(m<sup>2</sup>·h)**

Subsequently, a chemical cleaning process was initiated (Timepoint B). The initial membrane permeability was measured at approximately 170 L/(m<sup>2</sup>·h·bar). The first cleaning-in-place (CIP) with a 1.2 g/L SDS solution restored the membrane permeability to approximately 200 L/(m<sup>2</sup>·h·bar). A second CIP with a 200 mg/L NaOCl solution further increased the permeability to approximately 210 L/(m<sup>2</sup>·h·bar) by the end of the cleaning step (Timepoint C). Filtration with an emulsified oil was then resumed. The membrane permeability showed a slight decrease over the first three cycles, then, a significant increase in fouling was observed until reaching a permeability below 50 L/(m<sup>2</sup>·h·bar) within the sixth cycle. The experiment was subsequently halted after 11 hours (Timepoint D) due to the pressure again exceeding the maximum allowable limit. A subsequent cleaning step was ineffective and did not restore any of the membrane permeability.

Figure 24 compares the membranes operation as standalone UF and as hybrid coagulant-UF with a coagulant dose of 1 mg/L of Nüscofloc FE. The surfactant-free emulsified oil at oil concentration of 10 mg/L were filtered through two pristine LM<sub>2</sub> modules. Both were



conducted in dead-end at constant flux of  $100 \text{ L}/(\text{m}^2\cdot\text{h})$ . The first experiment was previously discussed and depicted in Figure 23. In the second experiment, which involved coagulation-UF operation, the membrane demonstrated a slight fouling, occurring at different rates, was observed in each cycle. For instance, during the second cycle, the membrane experienced a permeability decline of about 7%. The permeability also dropped to around  $385 \text{ L}/(\text{m}^2\cdot\text{h}\cdot\text{bar})$  and  $350 \text{ L}/(\text{m}^2\cdot\text{h}\cdot\text{bar})$  after 6 and 12 hours, which corresponds to the total fouling of about 18% and 26% respectively.

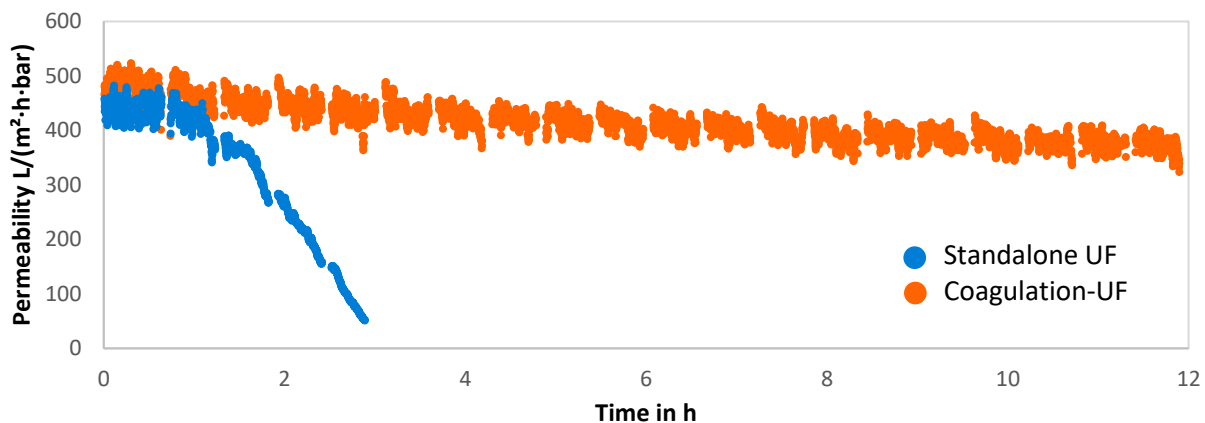


**Figure 24:** Permeability of filtering surfactant-free emulsified oils at oil concentration of  $10 \text{ mg}/\text{L}$  through  $\text{LM}_2$  modules as standalone UF or hybrid coagulant-UF. Nüscofloc FE was dosed as  $1 \text{ mg}/\text{L}$ . Both experiments were done at constant flux of  $100 \text{ L}/(\text{m}^2\cdot\text{h})$

Backwashing was not effective in significantly restoring membrane permeability. This fouling rate is comparable to that observed in experiments with SM modules, as depicted in Figure 21 (section 3.3.3.3), where the membrane lost between 1-4% of its permeability within a 45-minute filtration cycle.

The experiment was extended to approximately 5.5 days (Figure 25). However, it could also not be carried out continuously and the experiment paused at several time points, indicated as points A-D in Figure 25. Timepoints A, B, and C correspond to brief experimental stops due to temporary pressure spikes exceeding the maximum allowed pressure. The experiment resumed immediately after these events without further actions.

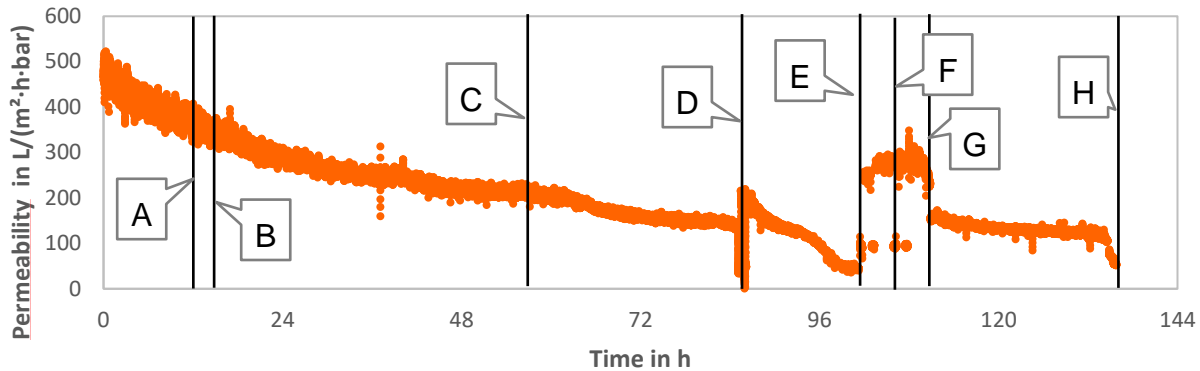


**Figure 25: Permeability of filtering surfactant-free emulsified oils at oil concentration of 10 mg/L through LM<sub>2</sub> module as hybrid coagulant-UF. Nüscofloc FE was dosed as 1 mg/L, flux was set constant to 100 L/(m<sup>2</sup>·h)**

Membrane performance showed a steady permeability decline. At around 86 hours (Timepoint D), a technical failure in the coagulation dosage pump led to a sharp permeability decline and pressure increase above the 2.5 bar limit, causing an automatic experiment abort. The membrane rested for about 12 hours before the issue was noticed. Several backwash steps partially restored permeability, and the experiment resumed with a permeability of about 200 L/(m<sup>2</sup>·h·bar).

Notably, the fouling rate increased post-resumption; permeability dropped from 200 to 140 L/(m<sup>2</sup>·h·bar) in less than four hours (Timepoints 86 to ~90 hours), a decline that previously took about 20 hours (Timepoints 60 to 80 hours). After 100 hours, the experiment stopped at timepoint E due to severe fouling, with permeability dropping below 50 L/(m<sup>2</sup>·h·bar) and pressure again exceeding 2.5 bar. A chemical cleaning at timepoint E (104.5 hours) restored permeability to 300 L/(m<sup>2</sup>·h·bar). A second chemical cleaning (Timepoint F) did not further improve permeability. Subsequent filtration of emulsified oil led to an immediate permeability decline to about 160 L/(m<sup>2</sup>·h·bar) followed by a steady decrease to 110 L/(m<sup>2</sup>·h·bar) after 134 hours, at which point the experiment stopped due to increased fouling and permeability falling below 50 L/(m<sup>2</sup>·h·bar).

The experiments demonstrate that coagulation dosing prior to UF membrane treatment effectively reduces the fouling rate and slightly enhances backwash efficiency, leading to improved overall membrane performance. These findings were validated at various scales, indicating good scalability of the results.

### 3 Conclusion and outlook

Investigations that were carried out in the W-UFO project were aligned in four topics: (1) Investigating the contribution of water-soluble oil fraction in the membrane fouling. (2) Further investigating the efficiency of surfactant-enhanced dead-end UF that was developed within the W-UFO II project. (3) Investigating the applicability of hybrid UF process, like combination with Powdered Activated Carbon (PAC) or coagulation: PAC-UF, coagulation-UF, and PAC-coagulation-UF. (4) Experiments relevant to practice for examining scalability of the results on longer membrane modules with increased active surface area and conduct long-term mini-plant experiments. Following conclusion can be made:

- 1- Our experiments revealed that dissolved crude oil components, i.e, WSO did not significantly contribute to the fouling of the UF membrane by emulsified oils under the tested conditions.
- 2- Further investigating the efficiency of surfactant-enhanced dead-end UF were conducted which can be summarized:
  - a. In results, three effects were found to be jointly responsible for the promoted hydraulic fouling reversibility and substantially improved mechanical backwashing efficiency via SDS dosing prior to membrane filtration: (i) the modification of emulsified oil droplets. (ii) The adsorption of SDS monomers into PES membrane matrix (below CMC) induced membrane surface hydrophilization and weakened oil adhesion by minimizing hydrophobic-hydrophobic interactions. (iii) the surfactant monomers in the formed fouling layer promoted the access of backwashing water through the fouling layer, decreased the interfacial surface tension between oil and water, and consequently, enhanced the backwashing efficiency.
  - b. Determining the SDS concentration in the permeate of the UF membrane was challenging. Four methods were examined based on literature: It was concluded that SDS was not retained by the UF membrane.
  - c. During the W-UFO project, three SDS products  $SDS_{VWR21}$ ,  $SDS_{VWR,23}$  and SDSTS were used. Notable differences were observed in PES membrane fouling during filtration of SDS-modified emulsified oils and oil-free SDS solutions. Filtration experiments with two types of capillary membranes from

- different manufacturers indicated that the SDS-enhanced dead-end UF method was sensitive to minor alterations in the quality of the applied SDS.
- d. Our experiments on optimizing operational conditions, including filtration flux, filtration duration, BW flux, and BW duration, did not lead to enhanced membrane performance. This may be attributed to the SDS type used (i.e., SDS<sub>VWR,23</sub>), which proved ineffective in restoring membrane performance through BW.
  - e. Higher carbon footprint was calculated for the surfactant-enhanced dead-end UF compared to the crossflow operation. The developed surfactant-enhanced dead-end UF was found less economically feasible than the cross-flow operation mode due to high costs associated to the procurement cost of the SDS.
- 3- The project also included investigations on the applicability of hybrid UF processes combined with Powdered Activated Carbon (PAC) or coagulation: PAC-UF, coagulation-UF, and PAC-coagulation-UF.
- a. Significant portion of the oil components from the emulsified oils were adsorbed on the PAC (up to 75%), a certain non-adsorbable part could be noticed. The adsorption most likely follows a multi-component adsorption isotherm. However, the adsorption isotherm could not be determined. A high fluctuation in the elimination rate could be observed during adsorption isotherm experiments. Adsorbable components were assumed adsorbed on the outer surface of the PAC particles. No significant difference could be noticed when using different PAC types. An isotherm equilibrium could be noticed after 24 hours.
  - b. Dosing iron-based and aluminum-based coagulants enhanced the oil elimination from the emulsions, which is expected mainly to be attributed to an increase the oil coalescence between oil droplets. Iron-based coagulant exhibited higher elimination rates than the aluminum based one.
  - c. Dosing PAC prior to UF membranes did not significantly reduce the fouling or enhance the backwash efficiency. Dosing coagulant prior to UF membranes reduced the fouling rate but did not improve the backwash efficiency.

Dosing both PAC and Coagulation prior to UF reduced the fouling but could not outperform the coagulation-UF operation.

- d. Dosing PAC slightly improved the separation performance of the membrane compared to standalone UF membrane, on the other hand dosing coagulation alone or combined with PAC prior UF exhibited better separation performance.
- 4- The project also encompassed experiments relevant to practice for examining scalability of the results on longer membrane modules with an increased active surface area. These experiments included long-term mini-plant trials lasting up to six days. The dosage of an iron-based coagulant at concentration of 1 mg/L prior to UF significantly enhanced membrane performance and reduced the fouling rate, allowing filtration to continue for up to 80 hours without requiring chemical cleaning. In contrast, standalone UF could only operate for less than three hours under similar conditions.

Based on the findings of the W-UFO research project, several areas for further improvement could be identified:

- **Effective Cleaning Strategies:** Establish effective cleaning strategies, including testing different cleaning agents, protocols, and intervals. Determine the critical permeability level below which cleaning efficiency is significantly reduced preventing sustainable membrane operation.
- **Coagulation-UF Operation Feasibility:** Investigate the feasibility of coagulation-UF operation with coagulants of varying quality or from different suppliers, and with membranes from different manufacturers.
- **Influence of PAC Size:** Study the effect of PAC size on its efficiency in removing oil components, reducing PES-UF membrane fouling, and increasing membrane backwashability.
- **Alternative Adsorbers:** Given that oil adsorption on PAC mainly occurs on the outer surface, conduct filtration experiments with non-activated carbon or other adsorbents.

- Filtration Experiments with SDS: Perform filtration experiments using high-quality SDS, like the type used in the CMC analysis (section 4.3.1.7).

These recommendations and identified research areas highlight the potential for improving the efficiency and sustainability of membrane treatment processes for oily produced water.

## 4 References

1. Tadros, T.F., *Emulsions: Formation, Stability, Industrial Applications*. 2016: Walter de Gruyter GmbH & Co KG.
2. Ebrahimi, M., et al., *Development and production of oil-in-water vehicles — sub-micron emulsion using tubular ceramic membranes*. *Desalination*, 2008. **224**(1): p. 40-45.
3. Idrees, H., et al., *Surface Modification of Ready-to-Use Hollow Fiber Ultrafiltration Modules for Oil/Water Separation*. *Chemie Ingenieur Technik*, 2021. **93**(9): p. 1408-1416.
4. Ebrahimi, M., et al., *Evaluation of the fouling potential of ceramic membrane configurations designed for the treatment of oilfield produced water*. *Separation Science and Technology*, 2018. **53**(2): p. 349-363.
5. Ebrahimi, M., et al., *Investigations on the use of different ceramic membranes for efficient oil-field produced water treatment*. *Desalination*, 2010. **250**(3): p. 991-996.
6. Ebrahimi, M., et al., *Characterization and application of different ceramic membranes for the oil-field produced water treatment*. *Desalination*, 2009. **245**(1): p. 533-540.
7. Dardor, D., et al., *Protocol for Preparing Synthetic Solutions Mimicking Produced Water from Oil and Gas Operations*. *ACS Omega*, 2021. **6**(10): p. 6881-6892.
8. Ahmad, T., C. Guria, and A. Mandal, *Optimal synthesis, characterization and antifouling performance of Pluronic F127/bentonite-based super-hydrophilic polyvinyl chloride ultrafiltration membrane for enhanced oilfield produced water treatment*. *Journal of Industrial and Engineering Chemistry*, 2020. **90**: p. 58-75.
9. Kumar, S., C. Guria, and A. Mandal, *Synthesis, characterization and performance studies of polysulfone/bentonite nanoparticles mixed-matrix ultrafiltration membranes using oil field produced water*. *Separation and Purification Technology*, 2015. **150**: p. 145-158.

10. Klemz, A.C., et al., *Oilfield produced water treatment by liquid-liquid extraction: A review*. Journal of Petroleum Science and Engineering, 2021. **199**: p. 108282.
11. Bandlien, E., et al., *Water Management in Oil and Gas Operations: Industry Practice and Policy Guidelines for Developing Countries*. International Development in Focus. 2024: The World Bank. 234.
12. Zheng, J., et al., *Offshore produced water management: A review of current practice and challenges in harsh/Arctic environments*. Marine Pollution Bulletin, 2016. **104**(1): p. 7-19.
13. Tummons, E.N., *Oil droplet behavior at the membrane surface during filtration of oil-water emulsions*. 2016, Michigan State University. p. 199.
14. Costa, T.C., et al., *Evaluation of the technical and environmental feasibility of adsorption process to remove water soluble organics from produced water: A review*. Journal of Petroleum Science and Engineering, 2022. **208**: p. 109360.
15. Liang, Y., et al., *Chapter Fourteen - Special Focus on Produced Water in Oil and Gas Fields: Origin, Management, and Reinjection Practice*, in *Formation Damage During Improved Oil Recovery*, B. Yuan and D.A. Wood, Editors. 2018, Gulf Professional Publishing. p. 515-586.
16. Eldos, H.I., et al., *Characterization and assessment of process water from oil and gas production: A case study of process wastewater in Qatar*. Case Studies in Chemical and Environmental Engineering, 2022. **6**: p. 100210.
17. Ekins, P., R. Vanner, and J. Firebrace, *Zero emissions of oil in water from offshore oil and gas installations: economic and environmental implications*. Journal of Cleaner Production, 2007. **15**(13): p. 1302-1315.
18. OSPAR-Commision. *Strategy of the OSPAR Comission for the Protection of the Marine Environment of the North-East Atlantic 2030*. Agreement 2021-02 2021; Available from: <https://www.ospar.org/convention/strategy/implementation-plan>.
19. Cordes, E.E., et al., *Environmental Impacts of the Deep-Water Oil and Gas Industry: A Review to Guide Management Strategies*. Frontiers in Environmental Science, 2016. **4**.
20. Jiang, W., et al., *Analysis of Regulatory Framework for Produced Water Management and Reuse in Major Oil- and Gas-Producing Regions in the United States*. Water, 2022. **14**(14): p. 2162.
21. Seager, R., et al., *Whither the 100th Meridian? The Once and Future Physical and Human Geography of America's Arid-Humid Divide. Part I: The Story So Far*. Earth Interactions, 2018. **22**(5): p. 1-22.



22. Amakiri, K.T., et al., *Physicochemical assessment and treatment of produced water: A case study in Niger delta Nigeria*. Petroleum Research, 2023. **8**(1): p. 87-95.
23. Owolabi, A. and P. Adesida, *ASSESSMENT OF THE PHYSICOCHEMICAL CHARACTERISTICS OF PRODUCED WATER IN SELECTED FLOW-STATIONS IN DELTA STATE, NIGERIA*. JOURNAL OF ENGINEERING AND ENGINEERING TECHNOLOGY, 2022.
24. Isehunwa, S. and S. Onovae, *Evaluation of produced water discharge in the Niger-Delta*. 2011.
25. Nwosi-Anele, A. and O. Iledare, *Produced Water Treatment Methods and Regulations: Lessons from the Gulf of Mexico and North Sea for Nigeria*. American Journal of Engineering Research, 2016. **5**: p. 46-57.
26. Cooper, C.M., et al., *Oil and Gas Produced Water Reuse: Opportunities, Treatment Needs, and Challenges*. ACS ES&T Engineering, 2022. **2**(3): p. 347-366.
27. Veil, J., *US produced water volumes and management practices in 2012*, in *Groundwater Protection Council*. 2015.
28. Yazdan, M.M.S., et al., *Review on the Evaluation of the Impacts of Wastewater Disposal in Hydraulic Fracturing Industry in the United States*. Technologies, 2020. **8**(4): p. 67.
29. Scanlon, B.R., et al., *Can we beneficially reuse produced water from oil and gas extraction in the U.S.?* Science of The Total Environment, 2020. **717**: p. 137085.
30. Wright, L.A., S. Kemp, and I. Williams, *'Carbon footprinting': towards a universally accepted definition*. Carbon Management, 2011. **2**(1): p. 61-72.
31. Scrucca, F., et al., *Carbon Footprint: Concept, Methodology and Calculation*, in *Carbon Footprint Case Studies: Municipal Solid Waste Management, Sustainable Road Transport and Carbon Sequestration*, S.S. Muthu, Editor. 2021, Springer Singapore: Singapore. p. 1-31.
32. IPCC, *Global Warming potential 2013*.
33. Yang, X. and B. Su, *Impacts of international export on global and regional carbon intensity*. Applied Energy, 2019. **253**: p. 113552.
34. Moro, A. and L. Lonza, *Electricity carbon intensity in European Member States: Impacts on GHG emissions of electric vehicles*. Transp Res D Transp Environ, 2018. **64**: p. 5-14.
35. Scarlat, N., M. Prussi, and M. Padella, *Quantification of the carbon intensity of electricity produced and used in Europe*. Applied Energy, 2022. **305**: p. 117901.



36. Nogueira, A.R., et al., *Environmental and energetic effects of cleaner production scenarios on the Sodium Lauryl Ether Sulfate production chain*. Journal of Cleaner Production, 2019. **240**: p. 118203.
37. EEA, E.e.a. *Greenhouse gas emission intensity of electricity generation* 2023 Sep., 13 [cited 2024 Mai, 22]; Available from: [https://www.eea.europa.eu/data-and-maps/daviz/co2-emission-intensity-14#tab-chart\\_7](https://www.eea.europa.eu/data-and-maps/daviz/co2-emission-intensity-14#tab-chart_7).
38. Lin, Y.-M. and G.C. Rutledge, *Separation of oil-in-water emulsions stabilized by different types of surfactants using electrospun fiber membranes*. Journal of Membrane Science, 2018. **563**: p. 247-258.
39. Matos, M., et al., *Surfactant effect on the ultrafiltration of oil-in-water emulsions using ceramic membranes*. Journal of Membrane Science, 2016. **520**: p. 749-759.
40. Trinh, T.A., et al., *Microfiltration of oil emulsions stabilized by different surfactants*. Journal of Membrane Science, 2019. **579**: p. 199-209.
41. Tummons, E., et al., *Membrane fouling by emulsified oil: A review*. Separation And Purification Technology, 2020. **248**: p. 116919.
42. Ma, Y., et al., *Investigation of Surfactant–Membrane Interaction Using Molecular Dynamics Simulation with Umbrella Sampling*. ACS ES&T Engineering, 2021. **1**(10): p. 1470-1480.
43. Hoeft, C.E. and R.L. Zollars, *Direct Determination of Anionic Surfactants Using Ion Chromatography*. Journal of Liquid Chromatography, 1994. **17**(12): p. 2691-2704.
44. Mateus, M.V., et al., *Molecular Interactions and Modeling of Anionic Surfactant Effect on Oxygen Transfer in a Cylindrical Reactor*. Environmental Engineering Science, 2018. **36**(2): p. 180-185.
45. Rupprecht, K.R., et al., *A precise spectrophotometric method for measuring sodium dodecyl sulfate concentration*. Analytical Biochemistry, 2015. **486**: p. 78-80.
46. DVGW, *Arbeitsblatt W 218. Flockung in der Wasseraufbereitung - Flockungstestverfahren*. 1988, DVGW Deutsche Vereinigung des Gas- und Wasserfachs e.V.: Bonn.

## 5 Appendices

### 5.1 List of Abbreviations

Abb.	Unit	Description
$A_i / A_0$	-	Relative integrated area of the respective peaks/ integrated area of the reference peaks in GC-MS Analysis
<b>BTEX</b>		Benzene, toluene, ethylbenzene, and xylene
<b>BW</b>		Hydraulic backwash
<b>C</b>	g/L	Concentration
<b>CFP</b>	kg CO <sub>2eq</sub>	Carbon footprint
<b>CFV</b>	m/s	Crossflow velocity
<b>CI</b>	kg CO <sub>2eq</sub>	Carbon Intensity
<b>CIP</b>		Cleaning-in-place
<b>CMC</b>	g/L	Critical micelle concentration
<b>DI</b>		Pure water
<b>D<sub>50,v</sub></b>	µm	Median droplet size of volume distribution; Diameter where 50% of the volume distribution has a smaller particle size
<b>DOC</b>	mg/L	Dissolved organic content
<b>EN</b>	kWh	Energy consumed by a pump
<b>EN<sub>s</sub></b>	kWh/m <sup>3</sup>	Specific energy consumption
<b>EPA</b>		United States environmental protection agency
<b>FEEM</b>		Fluorophotometer with emission-excitation matrix
<b>FT-IR</b>		Fourier transform infrared
<b>HPH</b>		High-pressure homogenizer
<b>MF</b>		Microfiltration
<b>NEAES</b>		North-East Atlantic Environment Strategy
<b>NF</b>		Nanofiltration
<b>OSPAR</b>		Convention for the Protection of the Marine Environment of the North-East Atlantic
<b>PAC</b>		Powdered activated carbon
<b>PAH</b>		Polycyclic aromatic hydrocarbon
<b>PES</b>		Polyethersulfone
<b>PW</b>		Produced water
<b>SDS</b>		Sodium dodecyl sulfate
<b>SEM</b>		Scanning electron microscopy
<b>TDS</b>	mg/L	Total dissolved solids
<b>TMP</b>	bar	Transmembrane pressure
<b>TOC</b>	mg/L	Total organic carbon
<b>TOG</b>	mg/L	Total oil and grease
<b>UF</b>		Ultrafiltration
<b>US</b>		Ultrasound
<b>USA</b>		United States of America
<b>UVi</b>	m <sup>-1</sup>	Ultraviolet spectral absorption coefficient, where i represents the measurement wavelength in nm
<b>V</b>	L/m <sup>2</sup>	specific filtered volume per membrane area

---

<b>WP</b>	Workpackage
<b>WSO</b>	Water-soluble oil fraction
<b><math>\eta_F</math></b>	The pump's yields

---

## 5.2 List of Figures

Figure 1: GC-MS analysis of surfactant-free emulsified oily feed with oil concentration of 25 mg/L as TOC ..... 24

Figure 2: Reference components of surfactant-free emulsified oil that were detected with the GC-MS analysis with their respective retention time, integrated area of the intensity peak and probability of the detected component compared to the NIST library. Presented as average of four trials with the min. and max. error bars ..... 25

Figure 3: Relative area  $A_i/A_0$ , integrated area of intensity peaks ( $A_i$ ) of the reference components in the permeate of S450 and S200 membranes related to the respective integrated area of the intensity peak of the feed ( $A_0$ ). Presented as average of two trials with the min. and max. error bars ..... 26

Figure 4: Relative area  $A_i/A_0$ , of the permeate of SM membranes, when filtering the permeates of S450 membranes through SM membrane. .... 26

Figure 7: Normalized permeability of SM<sub>1</sub> membranes during single-cycle filtration experiment with the permeates of S100, S200 and S450 as feed ..... 27

Figure 9: Representation for the proposed joint effects induced by SDS dosing prior to ultrafiltration that are responsible for the substantially improved membrane antifouling performance vs. strong membrane fouling caused by dead-end ultrafiltration of SDS-free emulsified oil..... 28

Figure 7: Normalized permeability curves for specially designed multiple-cycle dead-end filtration tests, starting with filtration of 0.48 g/L oil-free SDS solution at a constant flux of 100 L/(m<sup>2</sup>·h) followed by filtration of surfactant-free emulsified oils (5 mg/L or 10 mg/L)..... 29

Figure 8: Calibration curve of measured UV<sub>453</sub> (m<sup>-1</sup>) against the SDS concentration (mg/L) for solutions prepared with two different background water matrices,

(A) ultrapure water and (B) permeate of 10 mg/L surfactant-free emulsified oil permeate through SM membrane ..... 31

Figure 9: Quantified SDS (mg/L) in the UF permeate against the filtration time (min) for (A) feed of 48 mg/L SDS without oil and (B) with emulsified oily feed at 10 mg/L as TOC through SM membranes ..... 32

Figure 12: Measured and calculated theoretical values for a pure SDS, and measured values for  $SDS_{VWR,23}$  and  $SDS_{TS}$  (Microanalytical Laboratory at University of Duisburg-Essen ) ..... 33

Figure 11: Normalized permeability curves for SM membranes in filtration tests with multiple-cycles at a constant flux of 100 L/(m<sup>2</sup>·h) using oil-free SDS solutions of different concentrations (0.024 - 1.2 g/L) made of (A)  $SDS_{VWR,21}$  and (B)  $SDS_{VWR,23}$ , ..... 34

Figure 12: Normalized permeability curve for filtering surfactant-modified emulsified oil with 10 mg/L and 25 mg/L both with 0.48 g/L of (A)  $SDS_{VWR,21}$  and (B)  $SDS_{VWR,23}$ . One trial each ..... 35

Figure 13: Normalized permeability curve for filtering (A) oil-free  $SDS_{TS}$  solutions and (B)  $SDS_{TS}$ -modified emulsified oil with oil concentration of 10 mg/L, both at SDS concentration of 0.24 g/L through SM membranes, one trial each..... 36

Figure 14: Normalized permeability curve for filtering (a) oil-free SDS solutions and (b) SDS-modified emulsified oil with oil concentration of 10 mg/L, both made with  $SDS_{VWR,23}$  at concentration of 0.24 g/L through SX membranes, one trial each ..... 37

Figure 15: Specific energy consumption of crossflow experiments with emulsified oils at concentration of 10, 25 and 50 mg<sub>TOC</sub>/L at CFV of 2.5 m/s. Calculated for  $\eta_F = 0.8$  (solid-colored) and 0.6 (hatched) ..... 40

Figure 16: Specific energy consumption of surfactant-enhanced dead-end UF experiments with surfactant-enhanced emulsified oils at a concentration of 10 mg/L with SDS concentration of 0.12, 0.48 and 1.2 g/L and an oil concentration of 25 and 50 mg/L with SDS concentration of 0.48 g/L. Calculated for  $\eta_F = 0.8$  (solid-colored) and 0.6 (hatched) ..... 41

Figure 14: Results of adsorption kinetic experiments of ABG-H, HMA-B and ORG-K PACs, presented as  $UV_{254}$  concentration in the permeate (C) related to the feed concentration( $C_0$ ) over time ..... 44

Figure 15:  $UV_{254}$  elimination in percentage against the direct dosed concentrations of three PACs, ABG-H, HMA-B and ORG-K to the emulsified oil of 25 mg/L as TOC, one trial each..... 45

Figure 19: Relative concentrations of oil as DOC and  $UV_{254}$  in the supernatant of the coagulation/flocculation experiments (C) related to the feed concentration( $C_0$ ) for Nüscofloc FE as iron-based coagulant and (b) Nüscofloc ALF as aluminum-based coagulant. Presented as average of two trials with the min. and max. error bars. .... 47

Figure 20: Normalized permeability curve of the dead-end filtration experiments on standalone S100, combination of coagulation-S100, PAC-S100 and coagulation-PAC-S100 for emulsified oils of 25 mg/L as TOC at constant pressure of 1 bar..... 48

Figure 21: Normalized permeability curve for filtering surfactant-free emulsified oil of 10 mg/L as TOC at constant pressure of 0.4 bar as standalone  $SM_1$  or as combination of coagulation- $SM_1$  with Nüscofloc FE coagulant at dosage of 1 mg/L..... 50

Figure 22: Elimination performance represented as percentage retention of  $UV_{254}$  for standalone S100, PAC-S100, coagulation-S100 and PAC-coagulation-S100 ..... 51

Figure 23: Permeability of filtering surfactant-free emulsified oils at oil concentration of 10 mg/L through  $LM_2$  membranes as standalone UF at constant flux of 100 L/( $m^2 \cdot h$ ) ..... 52

Figure 24: Permeability of filtering surfactant-free emulsified oils at oil concentration of 10 mg/L through  $LM_2$  modules as standalone UF or hybrid coagulant-UF. Nüscofloc FE was dosed as 1 mg/L. Both experiments werde done at constant flux of 100 L/( $m^2 \cdot h$ ) ..... 53

Figure 25: Permeability of filtering surfactant-free emulsified oils at oil concentration of 10 mg/L through LM<sub>2</sub> module as hybrid coagulant-UF. Nüscofloc FE was dosed as 1 mg/L, flux was set constant to 100 L/(m<sup>2</sup>·h) ..... 54

### 5.3 List of Tables

Table 1: Specifications for flat sheet membranes employed in this project.....	19
Table 2: Specifications for capillary membrane modules employed in this project .....	20
Table 3: A list of experiments completed in accordance with the statistical experimental plan with central composite design and the associated filtration flux, filtration cycle duration, backwash flux, backwash duration, and pure water filtration including experiments done on playground, number of successful cycle and total fouling.....	38
Table 4: Electricity price, the respective value for $\Delta\text{Cost}_{\text{EN}}$ considering an energy consumption of 0.778 kWh/m <sup>3</sup> and the $\Delta\text{Cost}$ considering an average SDS cost of 0,264 €/m <sup>3</sup> for Germany. Saudi Arabia, Egypt and Sweden.....	42